Spacetime Interfacial Damage Model for Dynamic Fracture in Brittle Materials

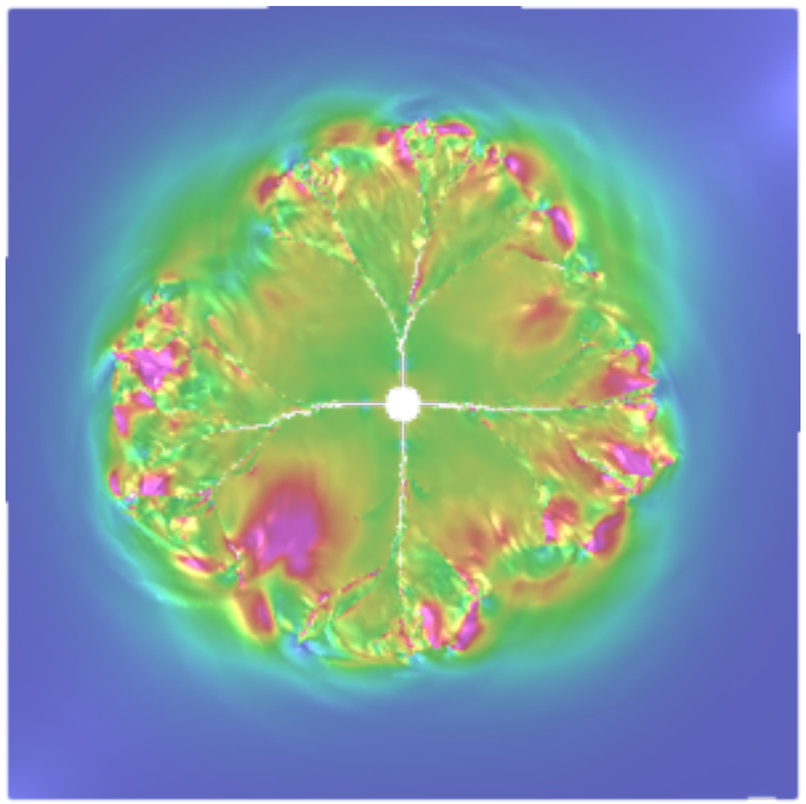

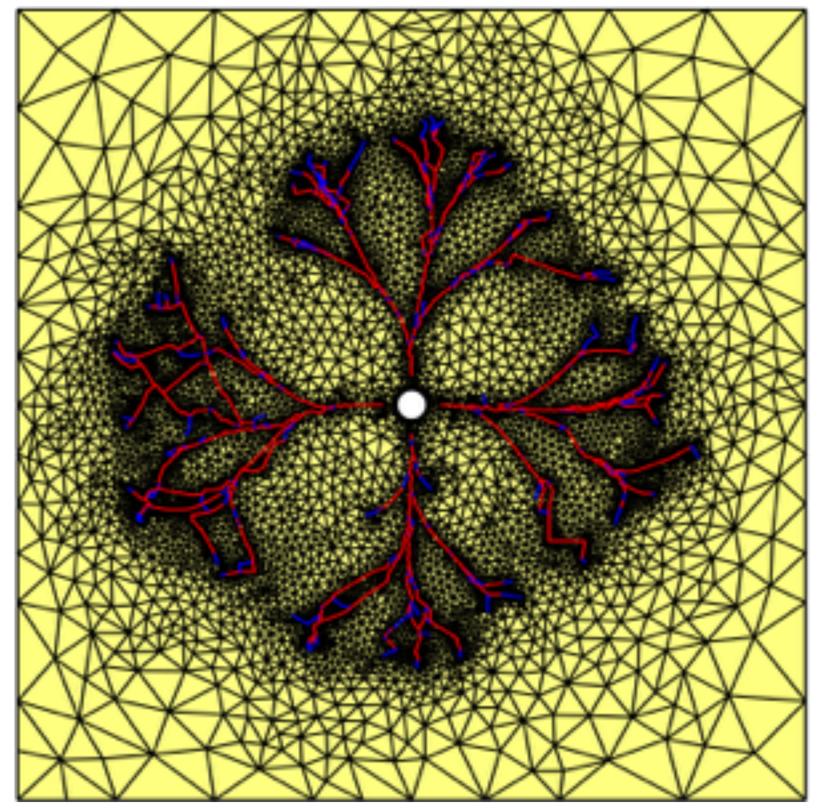

R. B. Haber[1] and R. Abedi[2]

[1]Mechanical Science & Engineering; University of Illinois at Urbana-Champaign

[2]Mechanical, Aerospace, & Biomedical Engineering; University of Tennessee Space Institute

Variational Models of Fracture

Banff International Research Station for Mathematical Innovation and Discovery

Alberta, CA — 8 - 13 May 2016

Catastrophe at the Tate Modern (London art museum)

Spacetime discontinuous Galerkin methods for hyperbolic systems

- Spacetime DG discretization
  - Replaces time integration
  - Ensures per-element conservation
  - Enforces weak spacetime jump conditions
  - Uses Riemann solutions for stability and to preserve characteristic structure
- ALE+
  - Unstructured grids graded in space and time
  - Powerful adaptive remeshing with no projections ensures high-order accuracy
  - No mesh tangling for moving boundaries
- Asynchronous solver
  - *O(N)* complexity
  - Scalable parallel meshing and local solves

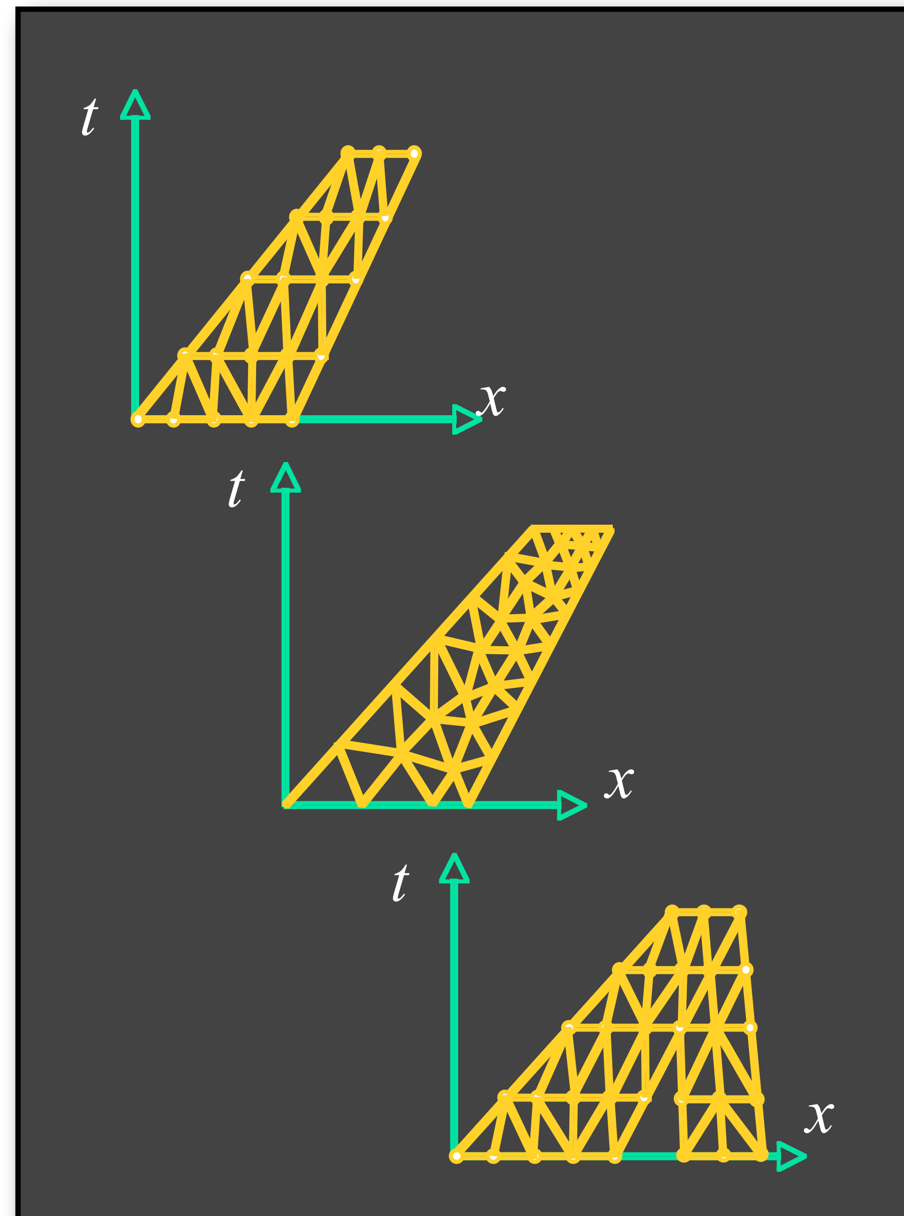

Causal Spacetime Mesh and O(*N*) Advancing-Front Solution Strategy

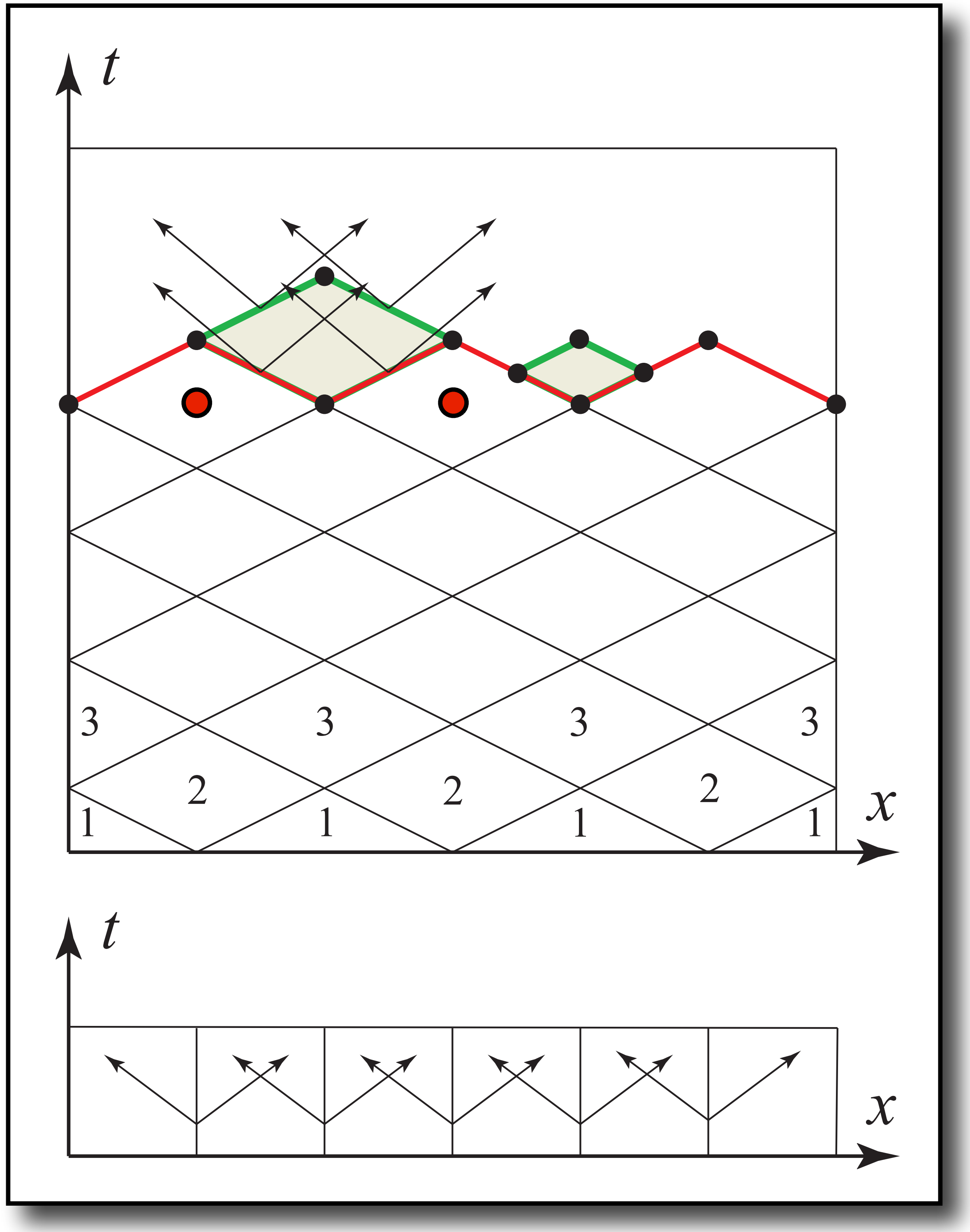

Tent Pitcher: causal spacetime meshing

- Given a space mesh, Tent Pitcher constructs a spacetime mesh such that every facet on sequence of advancing fronts is spacelike (patch height bounded by *causality constraint*)
- Similar to CFL condition, except entirely *local* and not related to stability (required for O(*N*) solution)

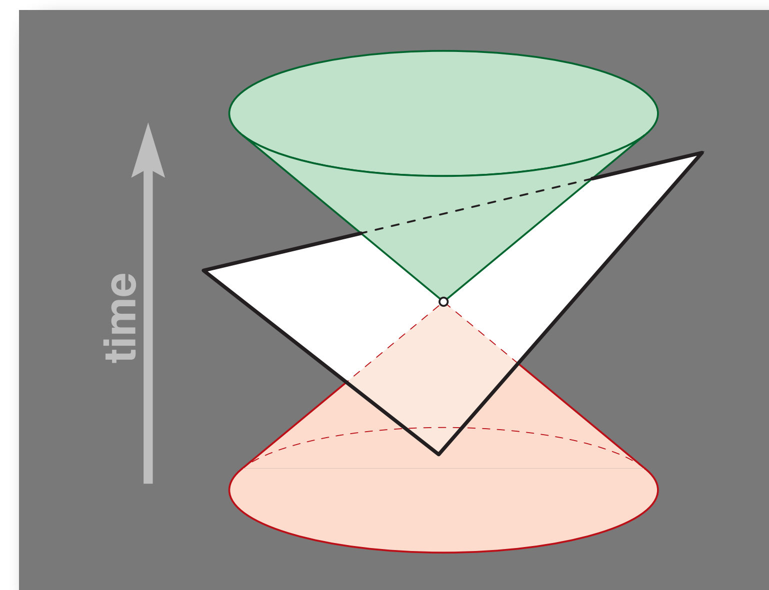

causality constraint

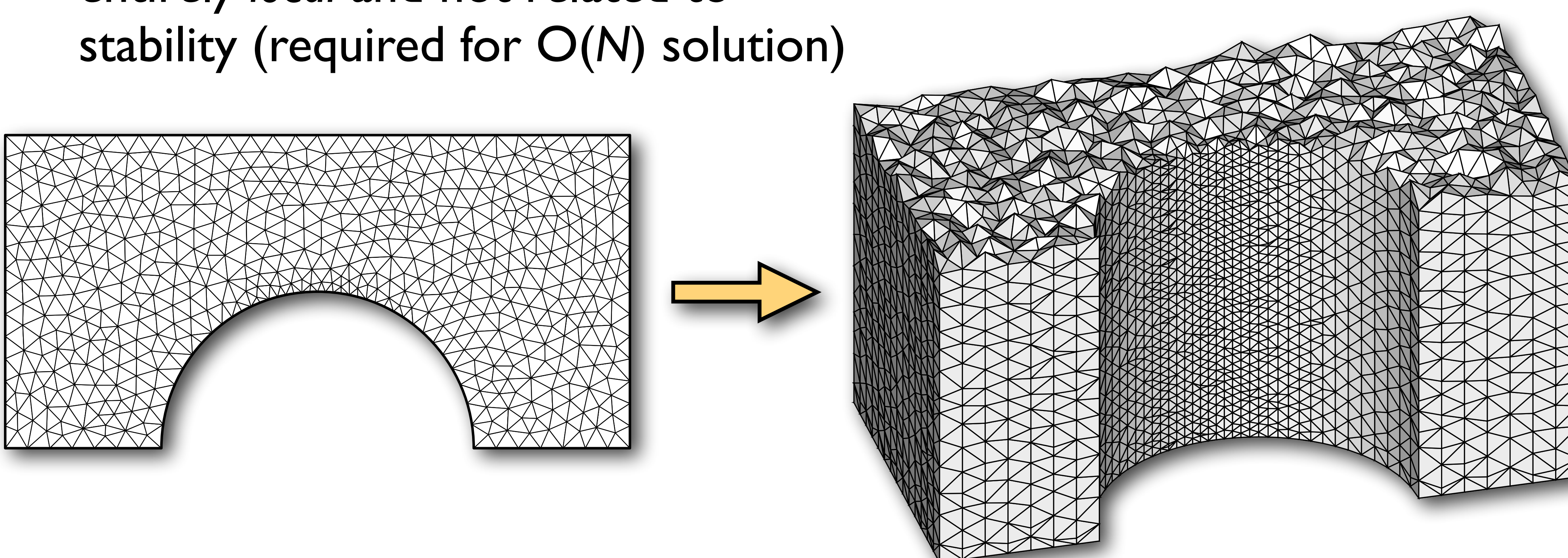

Tent Pitcher: patch–by–patch meshing & solution

- Patches ('tents') of tetrahedra; solve immediately for O(N) method with rich parallel structure
- Maintain "space mesh" as advancing, space-like front with non-uniform time coordinates

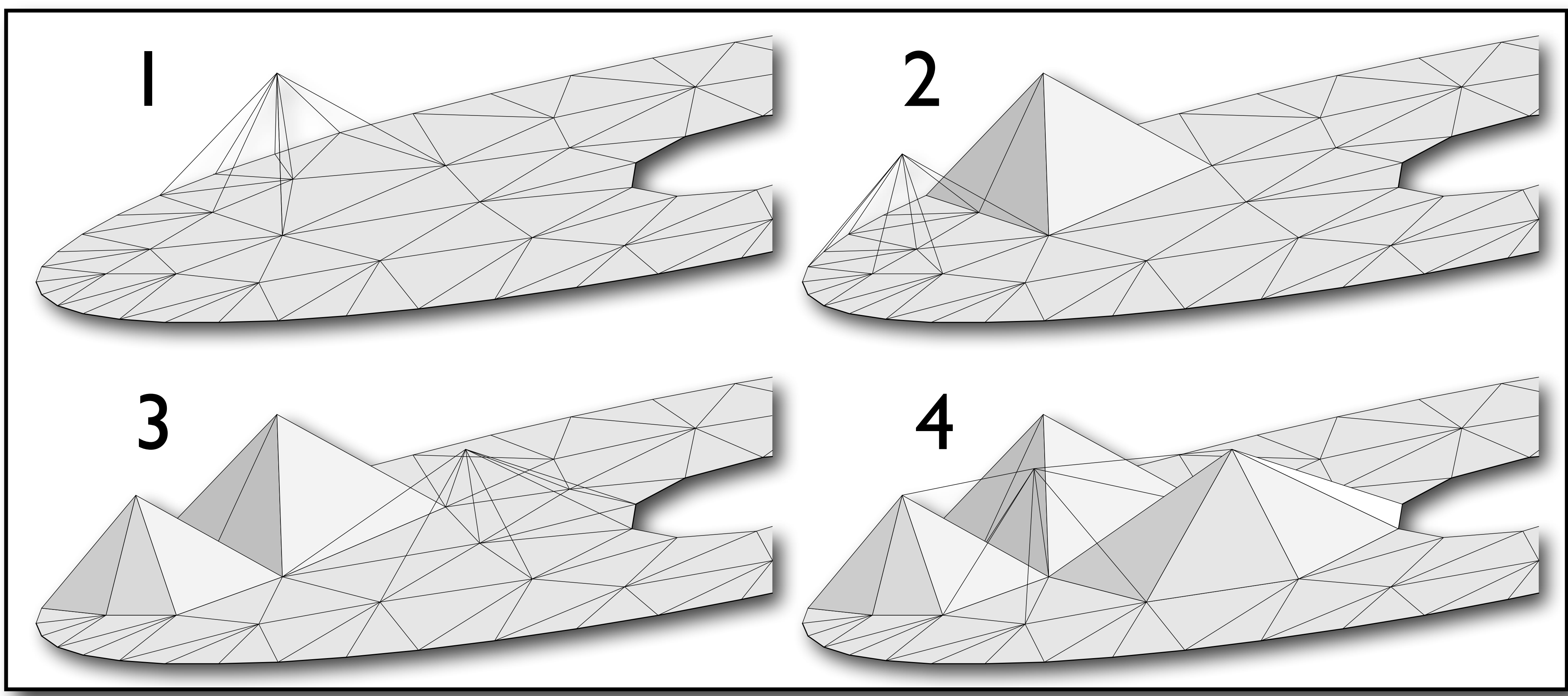

Adaptive refinement

- *Newest vertex refinement* of space mesh maintains element quality
- Supports nonconforming spacetime meshes

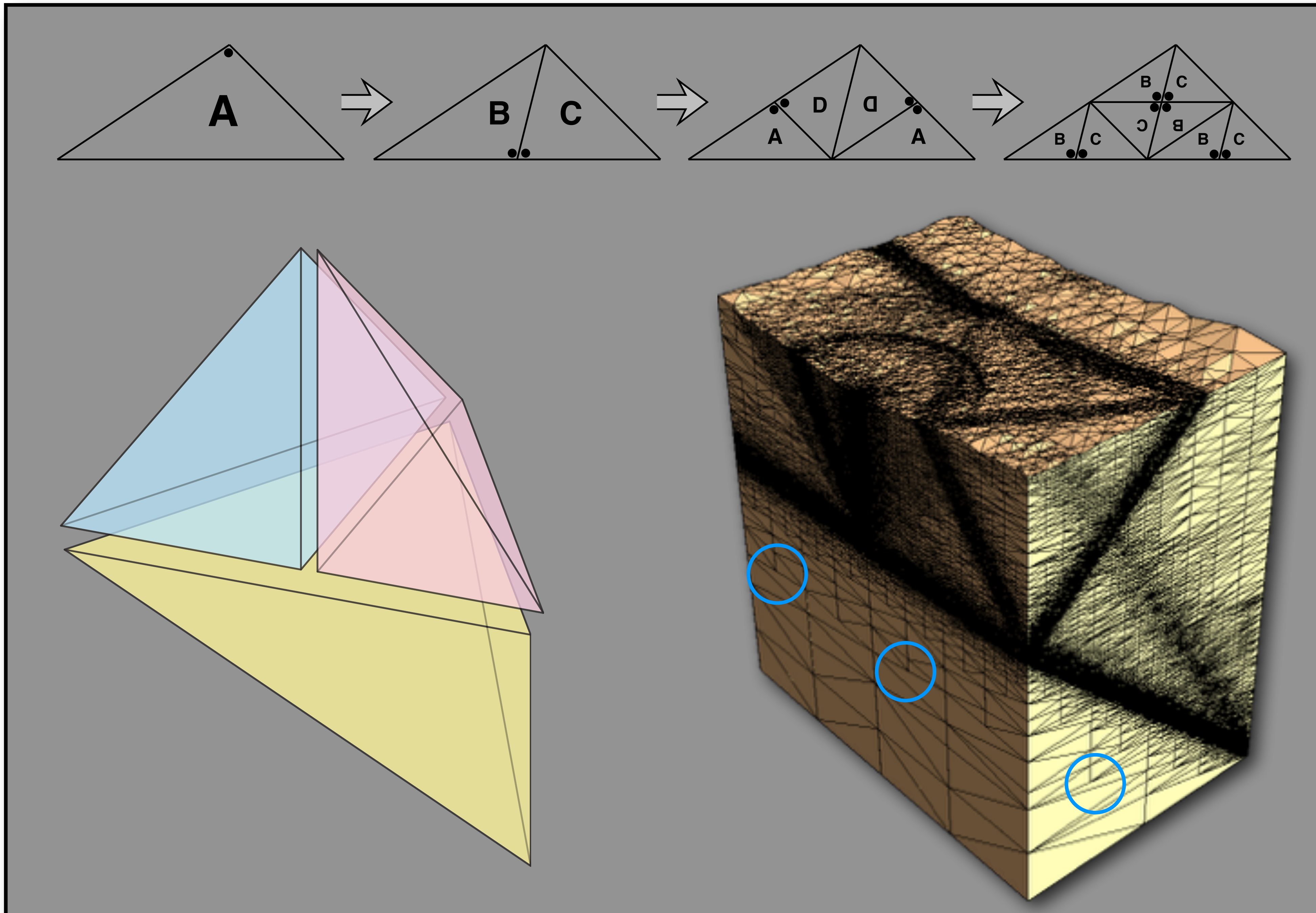

Spacetime adaptive meshing operations

- New spacetime adaptive meshing operations:
  - Vertex deletion (coarsening); Edge flip; Inclined tent poles (ALE, smoothing, tracking and repositioning)
  - Spacetime format eliminates projection error
  - Preserves high-order accuracy during remeshing

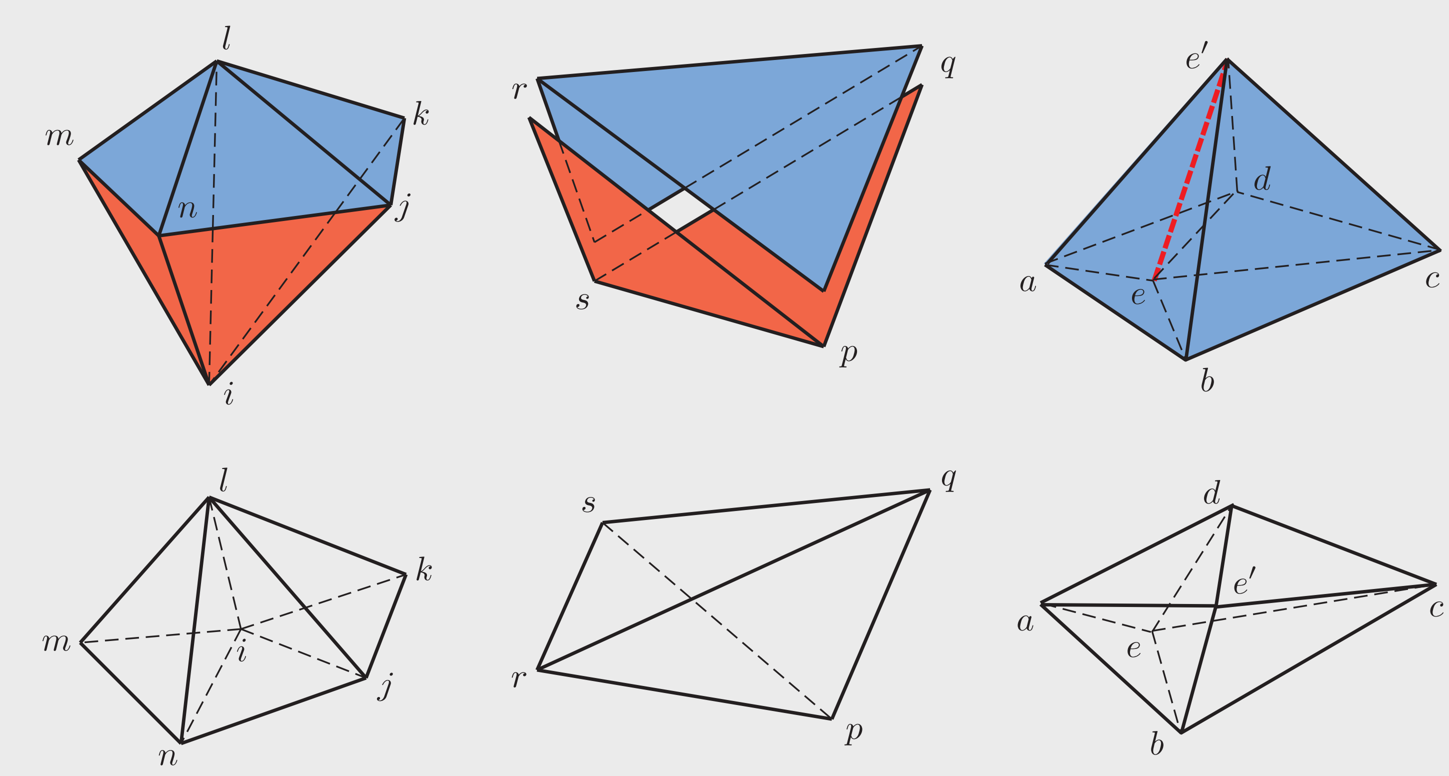

(a) Vertex deletion (degree 5) (b) Edge flip (c) Inclined tent pole

Crack-tip Wave Scattering

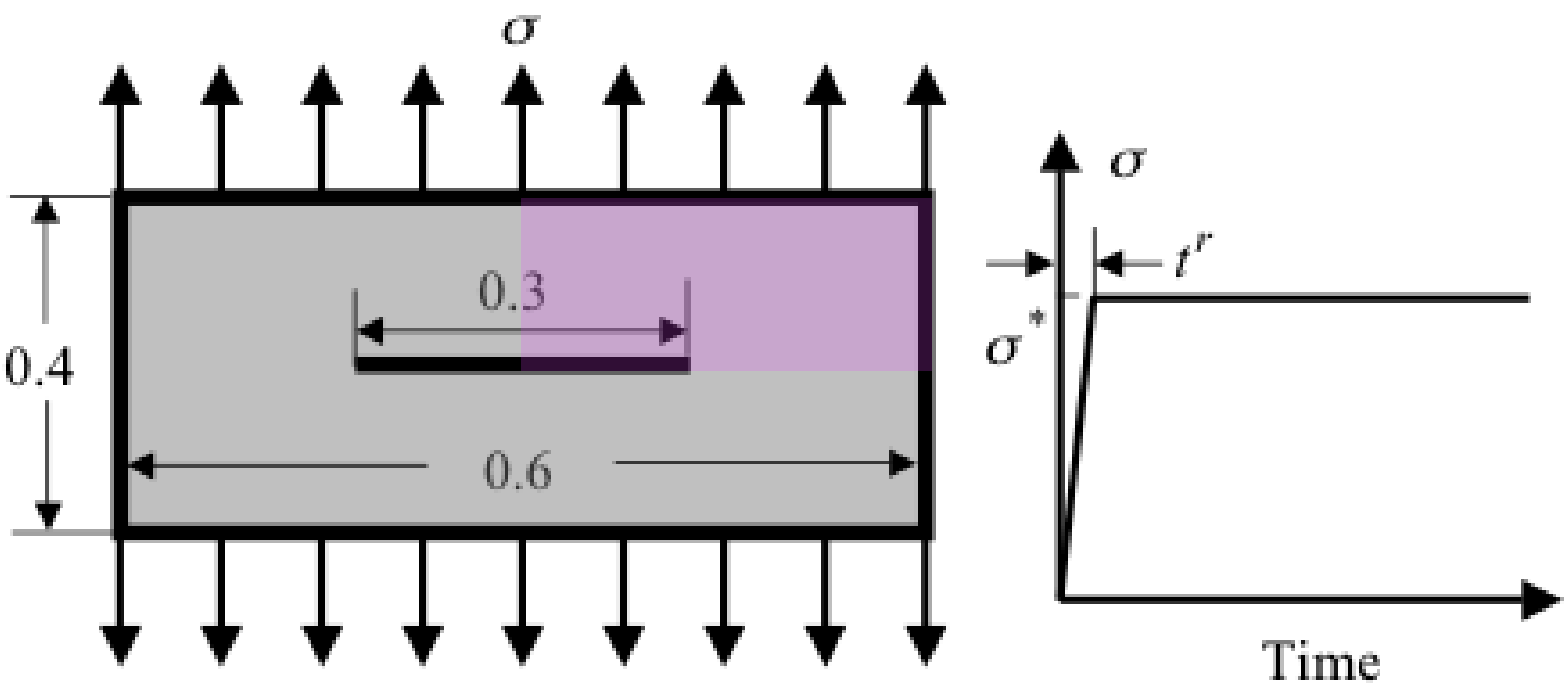

Crack-tip Wave Scattering

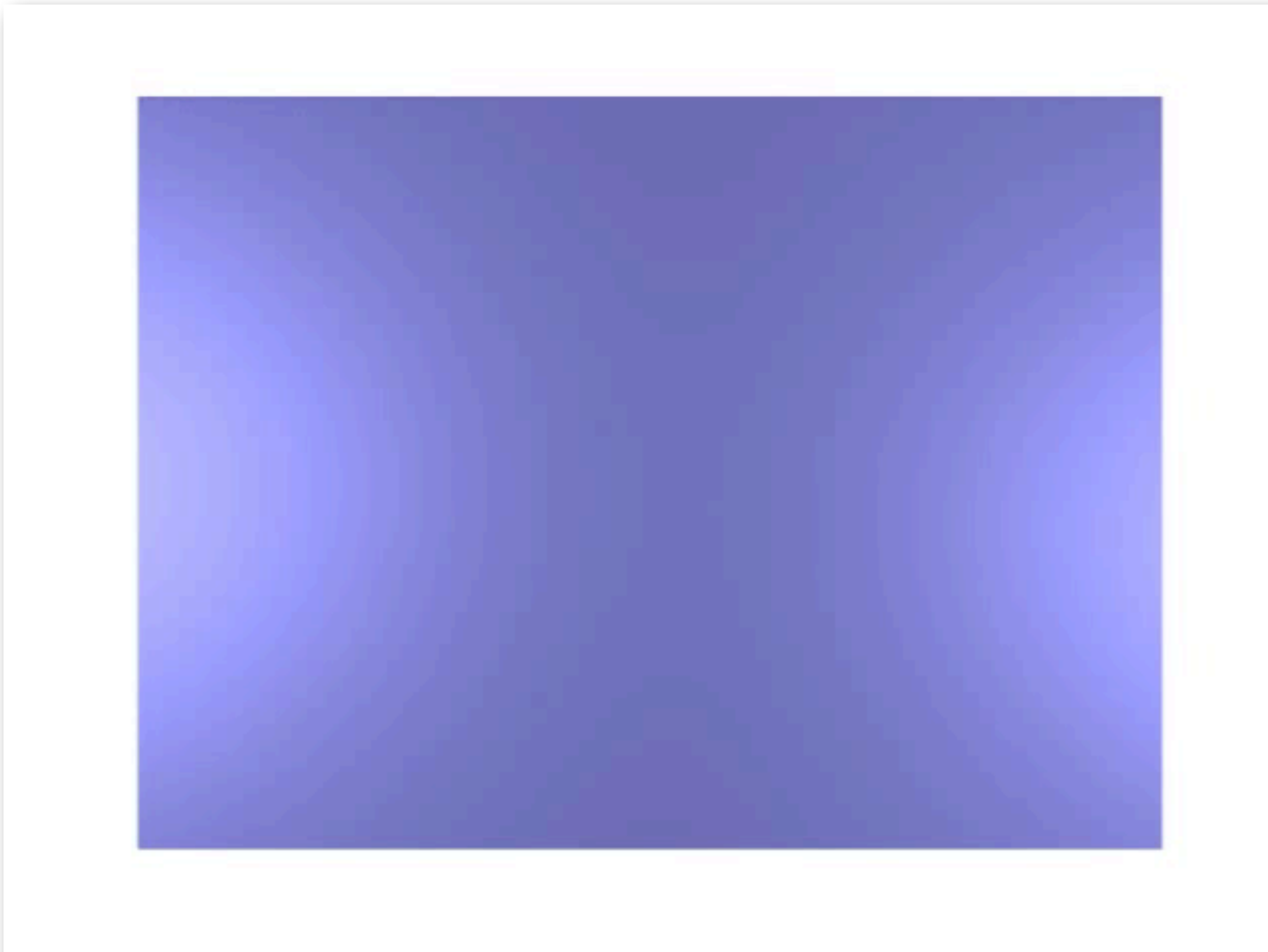

Crack-tip Wave Scattering

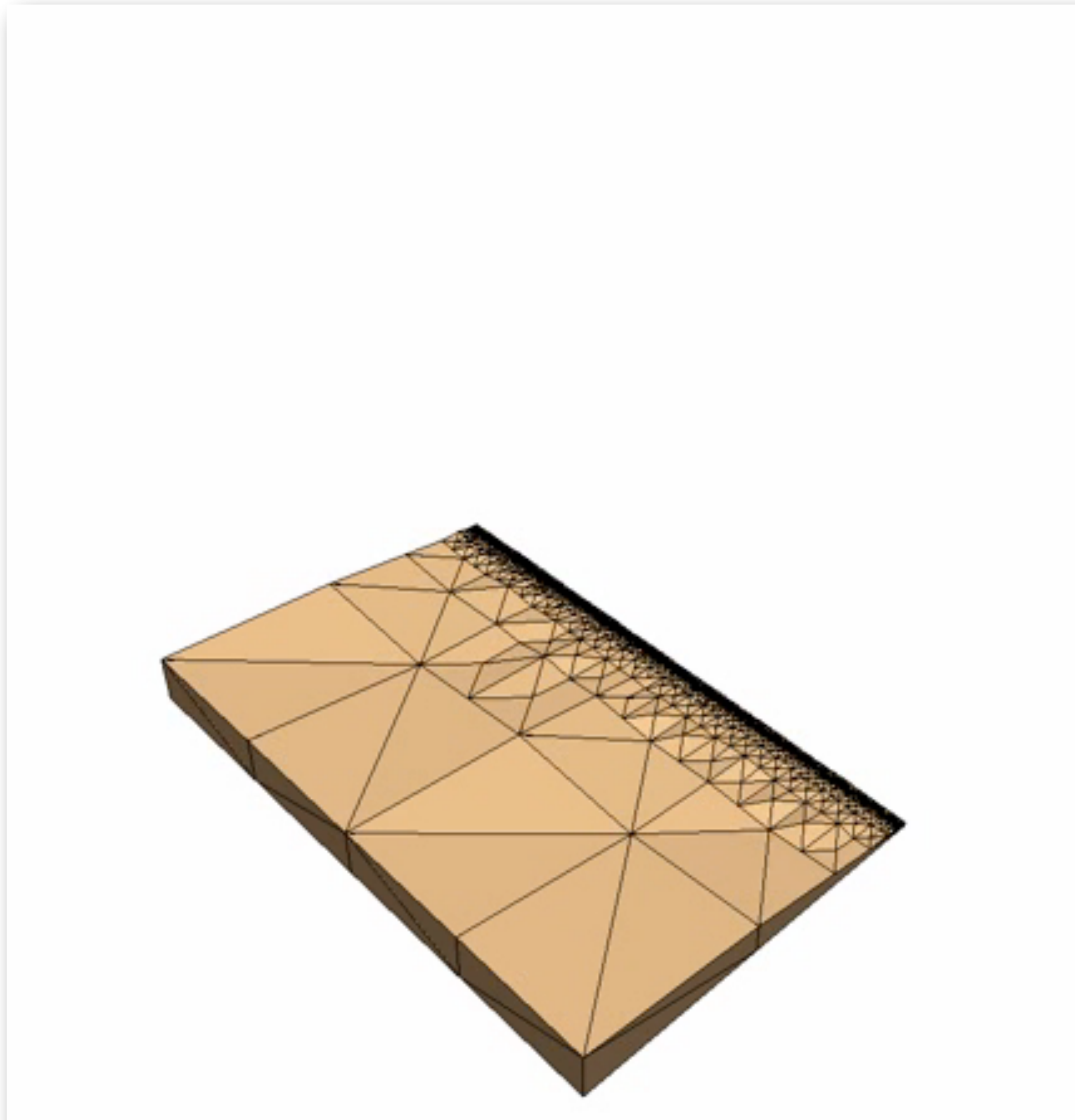

Crack-tip Wave Scattering

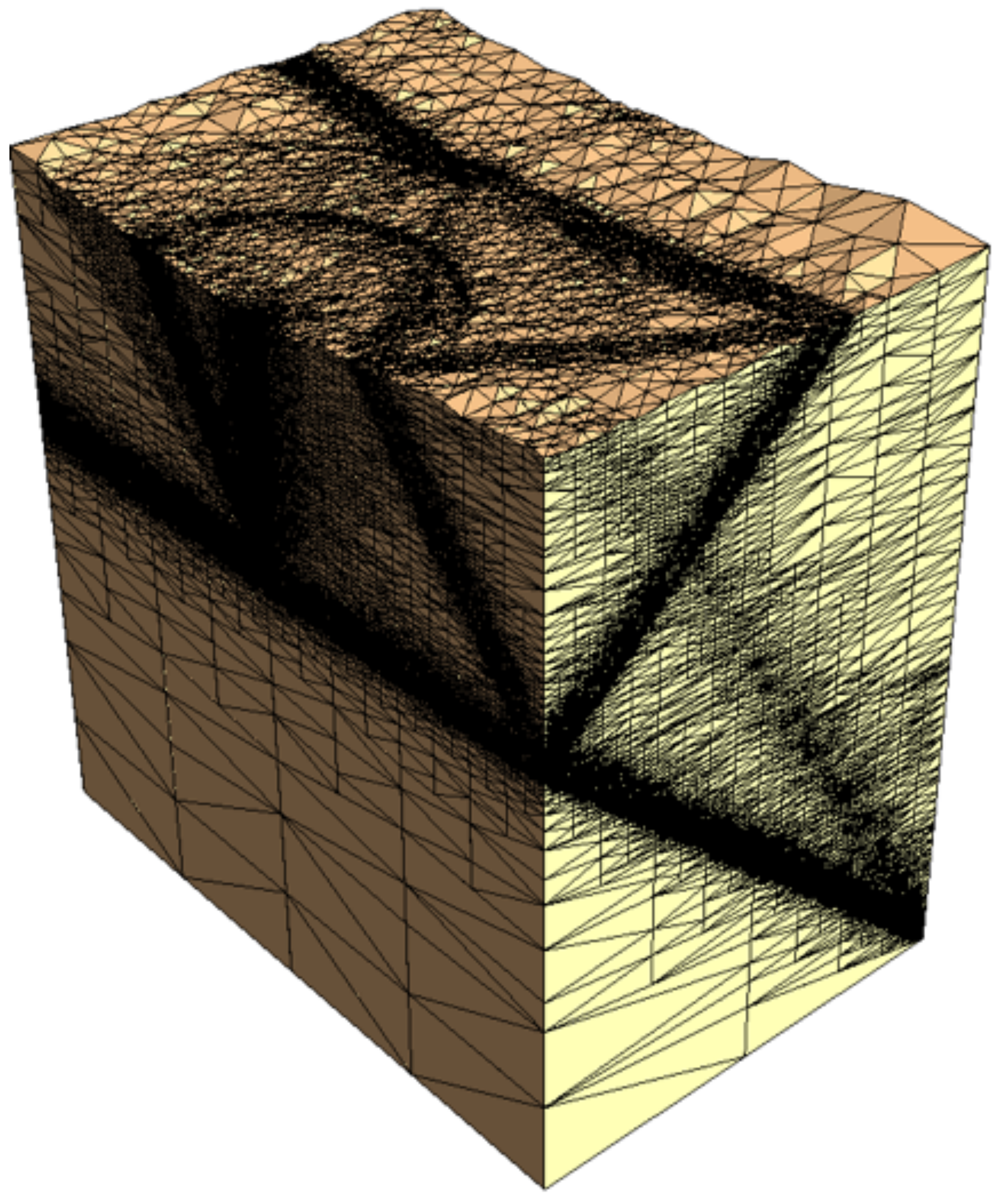

Near-perfect parallel scaling

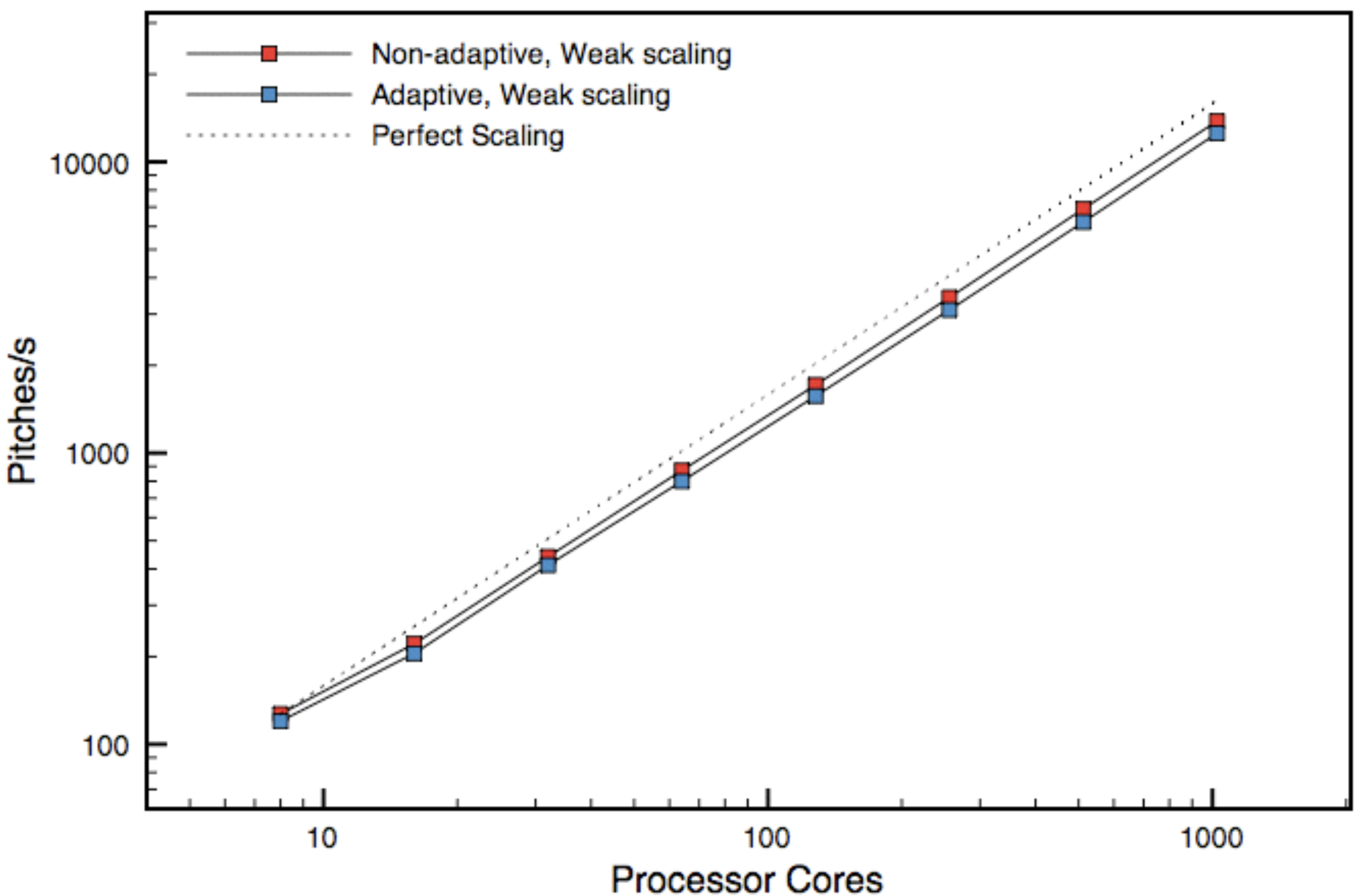

Spacetime fields

[*0, 1, d, and (d+1)*-forms]

- Displacement (0-form): $\mathbf{u}$
- Strain-velocity (1-form): $\boldsymbol{\varepsilon} := \boldsymbol{E} + \boldsymbol{v}$
  - Linearized strain + velocity
- Spacetime Momentum Flux (d-form): $\boldsymbol{M} := \boldsymbol{p} - \boldsymbol{S}$
  - Linear momentum density - stress
- Body force density ($(d+1)$-form): $\boldsymbol{b}$

Momentum Balance

- Integral form of linear momentum balance:

$$\begin{aligned} \int_{\partial Q} \boldsymbol{M} &= \int_Q \rho \boldsymbol{b} \quad \forall Q \subset D \\ \int_Q (\boldsymbol{dM} - \rho \boldsymbol{b}) &= \mathbf{0} \quad \forall Q \subset D \qquad \text{(Stokes Thm.)} \end{aligned}$$

- Local form with jump part:

$$\begin{aligned} (\boldsymbol{dM} - \rho \boldsymbol{b})|_{D \setminus \Gamma^{\mathrm{J}}} &= \mathbf{0} \\ [\![\boldsymbol{M}]\!]|_{D \cap \Gamma^{\mathrm{J}}} &= \mathbf{0} \mapsto (\boldsymbol{M}^* - \boldsymbol{M})|_{Q \cap \Gamma^{\mathrm{J}}} = \mathbf{0} \\ \boldsymbol{M}^* &= \text{Riemann or prescribed value} \end{aligned}$$

Kinematic compatibility

- Displacement-strain-velocity:

$$\boldsymbol{d}\mathbf{u} - \boldsymbol{\varepsilon} = \mathbf{0} \text{ in } \mathcal{V}^*_{\boldsymbol{M}} \ (\boldsymbol{\varepsilon} \text{ is exact})$$
$$[\![\mathbf{u}]\!]\,|_{D\cap\Gamma^{\mathrm{J}}} = \mathbf{0} \mapsto (\mathbf{u}^* - \mathbf{u})|_{D\cap\Gamma^{\mathrm{J}}} = \mathbf{0}$$

- Admissible strain-velocity:

$$\boldsymbol{d}\boldsymbol{\varepsilon} = \mathbf{0} \text{ in } \mathcal{V}^*_{\boldsymbol{iM}} \ (\boldsymbol{\varepsilon} \text{ is closed})$$
$$[\![\boldsymbol{\varepsilon}]\!]\,|_{D\cap\Gamma^{\mathrm{J}}} = \mathbf{0} \mapsto (\boldsymbol{\varepsilon}^* - \boldsymbol{\varepsilon})|_{D\cap\Gamma^{\mathrm{J}}} = \mathbf{0}$$
$$\boldsymbol{\varepsilon}^* = \text{Riemann or prescribed value}$$

1-field SDG formulation

Problem (Weighted residual form). *Find* $\mathbf{u} \in \mathcal{V}_{\mathbf{u}} \ni$

$$\int_{\mathcal{Q}} \mathbf{i}\hat{\boldsymbol{\varepsilon}} \wedge (\mathbf{d}\boldsymbol{M} - \rho\boldsymbol{b})$$

$$+ \int_{\partial\mathcal{Q}} \left[\mathbf{i}\hat{\boldsymbol{\varepsilon}} \wedge \left(\overset{\star}{\boldsymbol{M}} - \boldsymbol{M} \right) + (\overset{\star}{\boldsymbol{\varepsilon}} - \boldsymbol{\varepsilon}) \wedge \mathbf{i}\hat{\boldsymbol{M}} + (\overset{\star}{\mathbf{u}} - \mathbf{u}) \wedge \hat{\boldsymbol{f}}_{\mathrm{I}} \right] = 0$$

$$\forall\ \hat{\mathbf{u}} \in \mathcal{V}_{\mathbf{u}}$$

Problem (Weak form). *Find* $\mathbf{u} \in \mathcal{V}_{\mathbf{u}} \ni$

$$-\int_{\mathcal{Q}} (\mathbf{d}\mathbf{i}\hat{\boldsymbol{\varepsilon}} \wedge \boldsymbol{M} + \mathbf{i}\hat{\boldsymbol{\varepsilon}} \wedge \rho\boldsymbol{b})$$

$$+ \int_{\partial\mathcal{Q}} \left[\mathbf{i}\hat{\boldsymbol{\varepsilon}} \wedge \overset{\star}{\boldsymbol{M}} + (\overset{\star}{\boldsymbol{\varepsilon}} - \boldsymbol{\varepsilon}) \wedge \mathbf{i}\hat{\boldsymbol{M}} + (\overset{\star}{\mathbf{u}} - \mathbf{u}) \wedge \hat{\boldsymbol{f}}_{\mathrm{I}} \right] = 0$$

$$\forall\ \hat{\mathbf{u}} \in \mathcal{V}_{\mathbf{u}}$$

in which weighting $\hat{\boldsymbol{f}}_{\mathrm{I}}$ is projection of $\hat{\mathbf{u}}$ into subspace of time-invariant, infinitesimal-rigid deformations.

3-field SDG formulation

Problem (Weighted residual form)**.** *For each* $\mathcal{Q} \in \mathcal{P}$*, find* $(\mathbf{u}, \boldsymbol{\varepsilon}) \in \mathcal{V}_{\mathbf{u}} \times \mathcal{V}_{\boldsymbol{\varepsilon}}$ *such that for every* $\mathcal{Q} \in \mathcal{P}$

$$\int_{\mathcal{Q}} \left[\mathbf{i}\hat{\boldsymbol{\varepsilon}} \wedge (\mathbf{d}\boldsymbol{M} - \rho\boldsymbol{b}) + \mathbf{d}\boldsymbol{\varepsilon} \wedge \mathbf{i}\hat{\boldsymbol{M}} + (\mathbf{d}\mathbf{u} - \boldsymbol{v}) \wedge \hat{\boldsymbol{f}} \right]$$
$$+ \int_{\partial\mathcal{Q}} \left[\mathbf{i}\hat{\boldsymbol{\varepsilon}} \wedge (\boldsymbol{M}^* - \boldsymbol{M}) + (\boldsymbol{\varepsilon}^* - \boldsymbol{\varepsilon}) \wedge \mathbf{i}\hat{\boldsymbol{M}} + (\mathbf{u}^* - \mathbf{u}) \wedge \hat{\boldsymbol{f}} \right] \quad = 0$$
$$\forall\ (\hat{\mathbf{u}}, \hat{\boldsymbol{\varepsilon}}) \in \mathcal{V}_{\mathbf{u}} \times \mathcal{V}_{\boldsymbol{\varepsilon}}$$

in which $\hat{\boldsymbol{f}} = k^{\mathcal{Q}} \mathbf{1}(\hat{\mathbf{u}}) \star \mathrm{dt}$.

Problem (Weak form)**.** *Find* $(\mathbf{u}, \boldsymbol{\varepsilon}) \in \mathcal{V}_{\mathbf{u}} \times \mathcal{V}_{\boldsymbol{\varepsilon}}$ *such that for every* $\mathcal{Q} \in \mathcal{P}$ *such that*

$$- \int_{\mathcal{Q}} \left[\mathbf{d}\mathbf{i}\hat{\boldsymbol{\varepsilon}} \wedge \boldsymbol{M} + \mathbf{i}\hat{\boldsymbol{\varepsilon}} \wedge \rho\boldsymbol{b} - \boldsymbol{\varepsilon} \wedge \mathbf{d}\mathbf{i}\hat{\boldsymbol{M}} + \mathbf{u} \wedge \mathbf{d}\hat{\boldsymbol{f}} + \boldsymbol{v} \wedge \hat{\boldsymbol{f}} \right]$$
$$+ \int_{\partial\mathcal{Q}} \left[\mathbf{i}\hat{\boldsymbol{\varepsilon}} \wedge \boldsymbol{M}^* + \boldsymbol{\varepsilon}^* \wedge \mathbf{i}\hat{\boldsymbol{M}} + \mathbf{u}^* \wedge \hat{\boldsymbol{f}} \right] \quad = 0$$
$$\forall\ (\hat{\mathbf{u}}, \hat{\boldsymbol{\varepsilon}}) \in \mathcal{V}_{\mathbf{u}} \times \mathcal{V}_{\boldsymbol{\varepsilon}}$$

Convergence of 1-field model

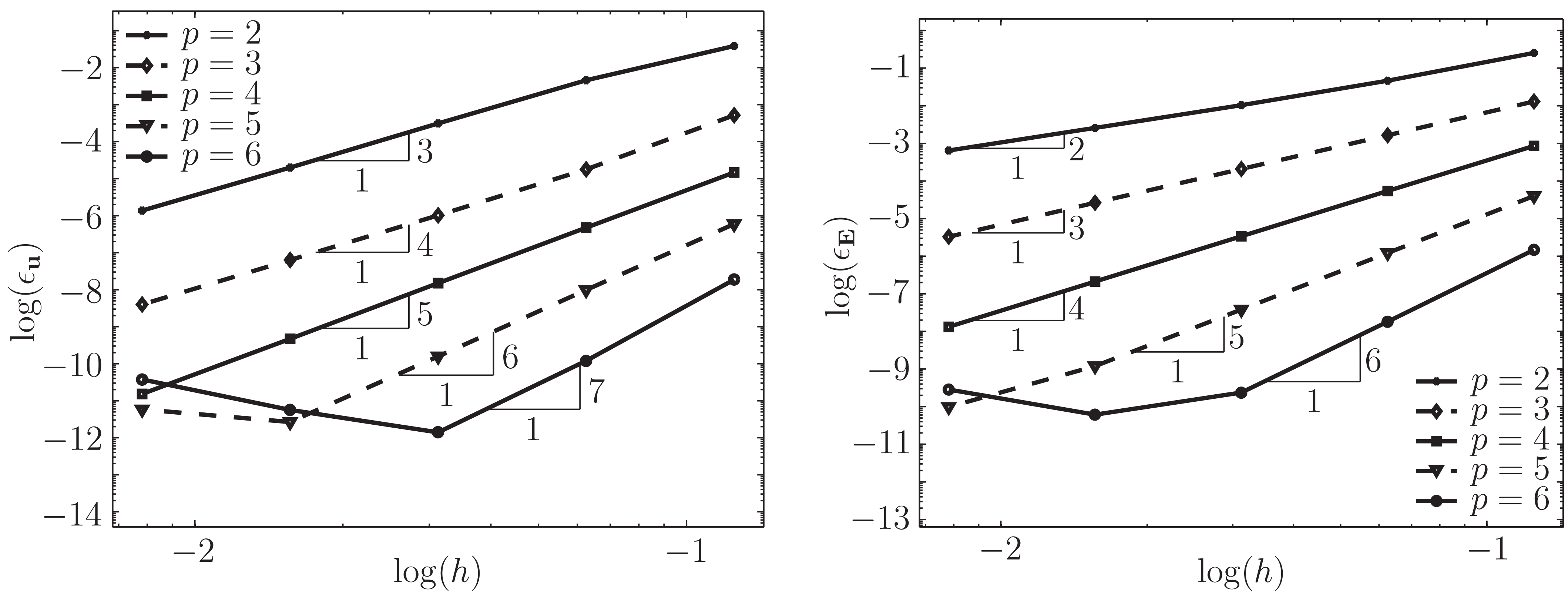

displacement strain (velocity)

Convergence of 3-field model

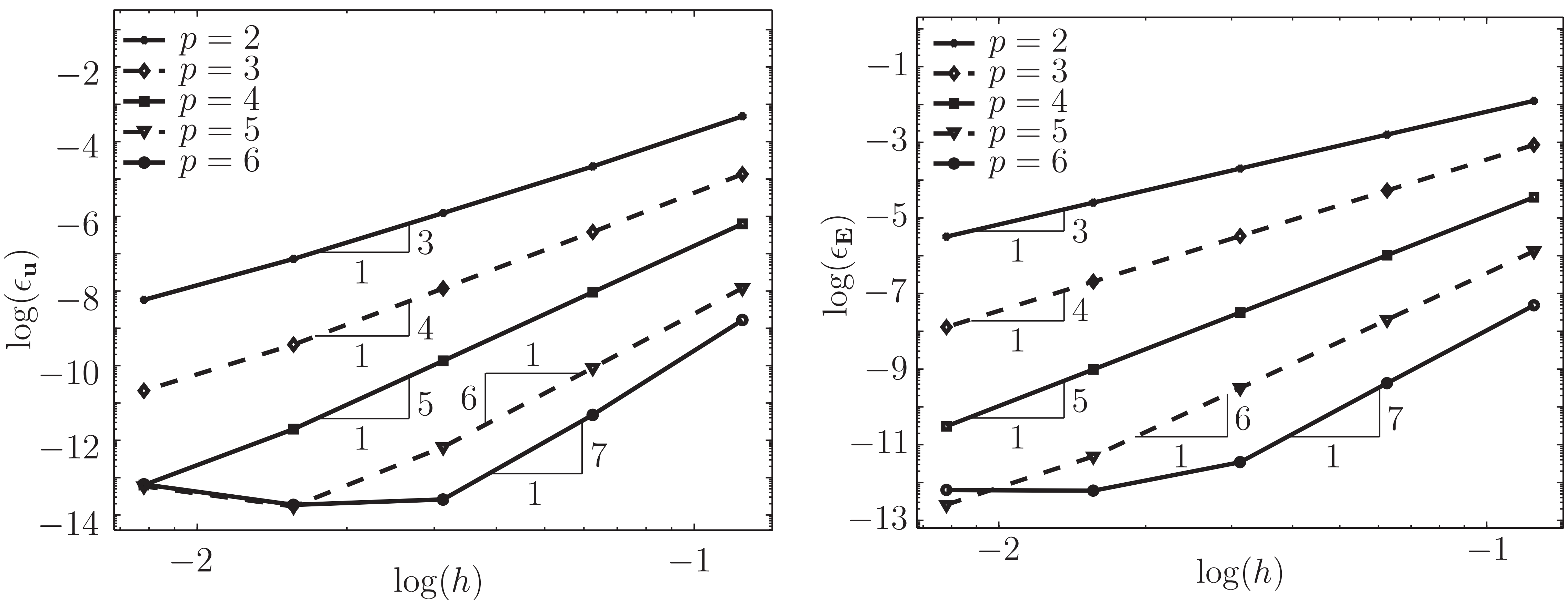

displacement   strain (velocity)

3-field model: optimal convergence in all three fields

Efficiency Study; *d*=2

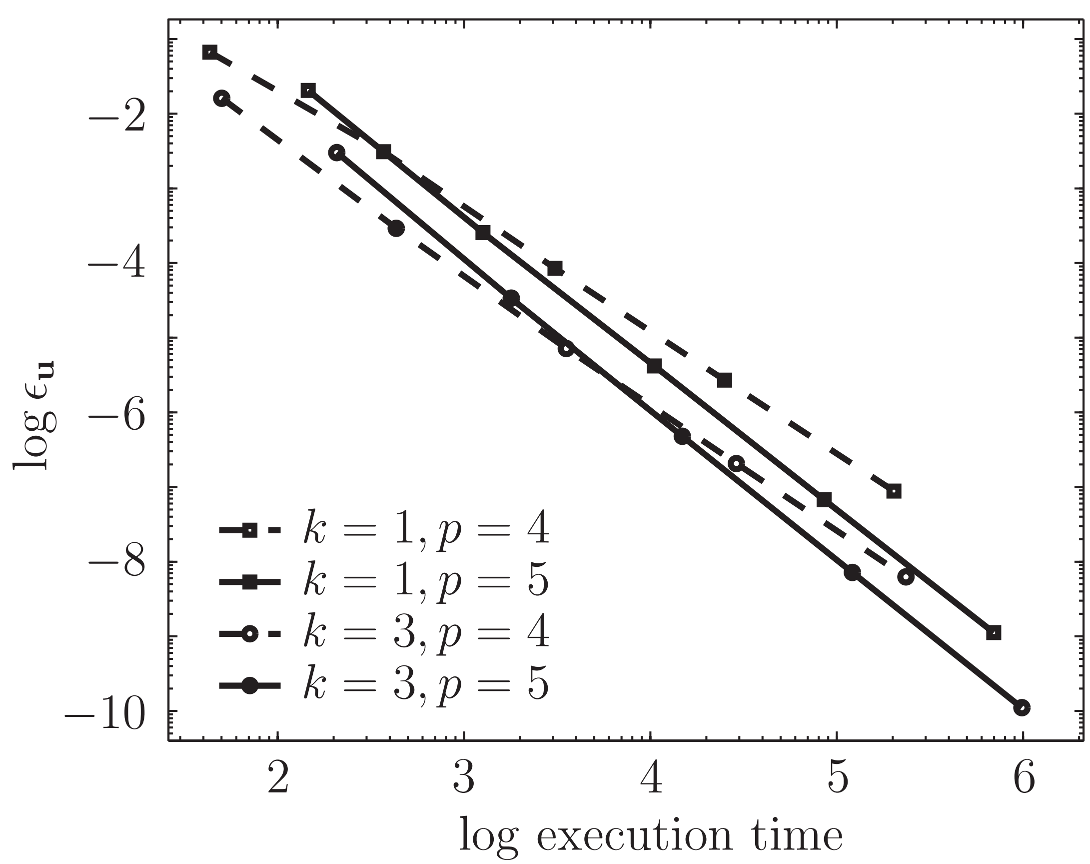

displacement

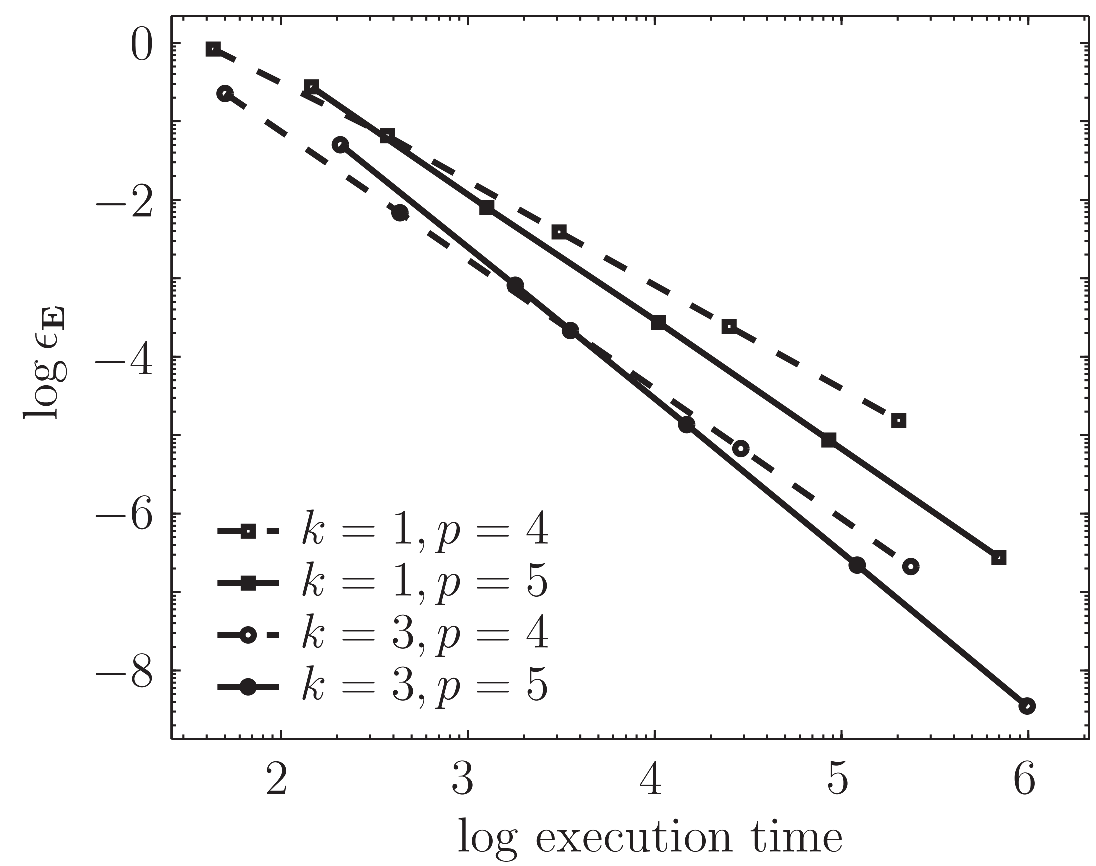

strain (velocity)

3-field model runs about 4x faster

Target Values: Initial/Boundary Conditions, Riemann Solutions, and Cohesive Model

- Unified framework preserves characteristic structure
- Simple extension to implement cohesive model

$$\boldsymbol{M}^* = \begin{cases} \boldsymbol{M} & \text{on outflow and prescribed-}\boldsymbol{\varepsilon}\text{ boundaries} \\ \bar{\boldsymbol{M}} & \text{on initial \& prescribed-}\boldsymbol{M}\text{ domain boundaries} \\ \boldsymbol{M}^+ & \text{on interior element inflow boundaries} \\ \boldsymbol{M}^{\mathrm{R}} & \text{on non-causal \& non-cohesive interior boundaries} \\ \boldsymbol{M}^{\mathrm{T}SL} & \text{on cohesive interfaces} \end{cases}$$

$$\boldsymbol{\varepsilon}^* = \begin{cases} \boldsymbol{\varepsilon} & \text{on outflow, prescribed-}\boldsymbol{M}\text{, \& cohesive boundaries} \\ \bar{\boldsymbol{\varepsilon}} & \text{on initial \& prescribed-}\boldsymbol{\varepsilon}\text{ domain boundaries} \\ \boldsymbol{\varepsilon}^+ & \text{on interior element inflow boundaries} \\ \boldsymbol{\varepsilon}^{\mathrm{R}} & \text{on non-causal \& non-cohesive interior boundaries} \end{cases}$$

Center–Cracked Tension Specimen

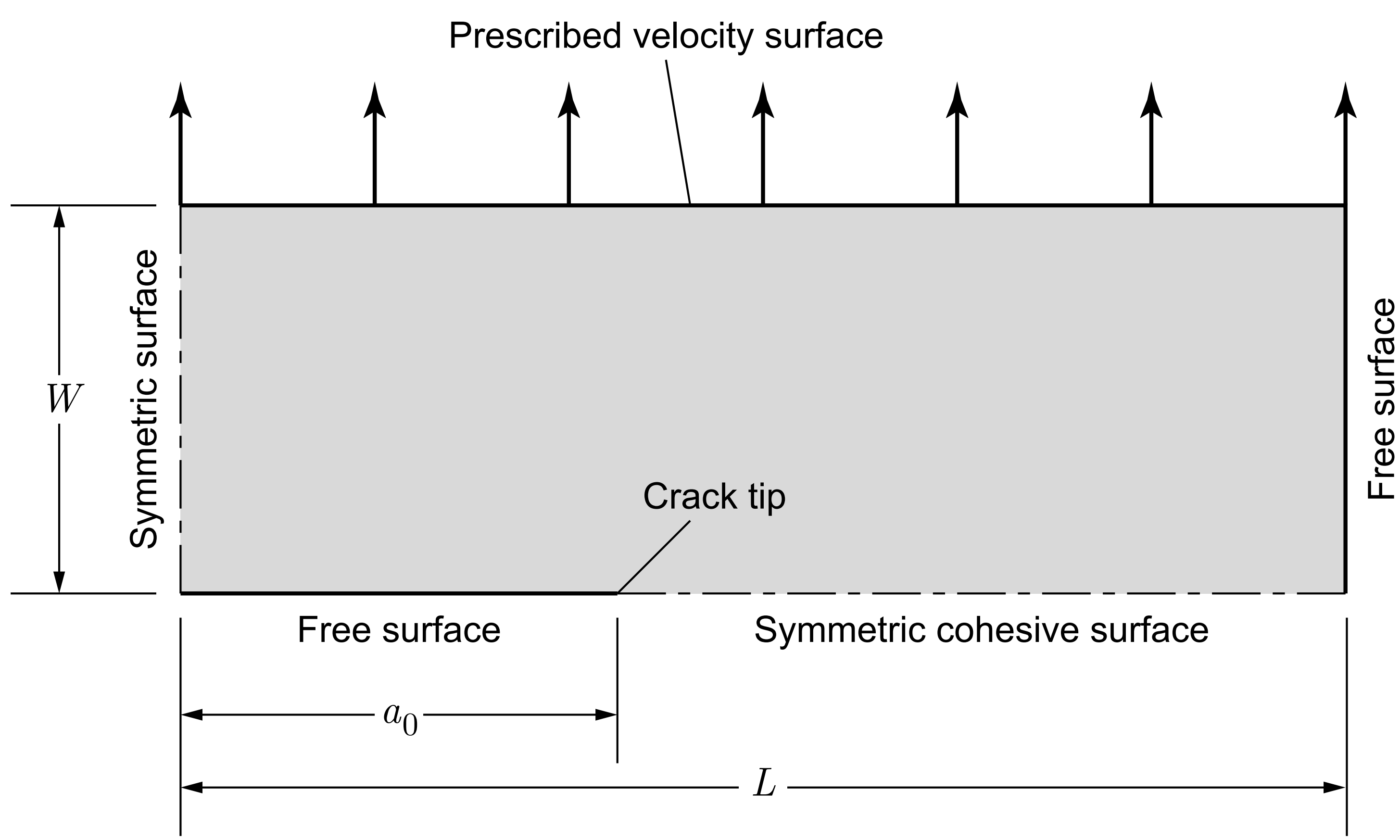

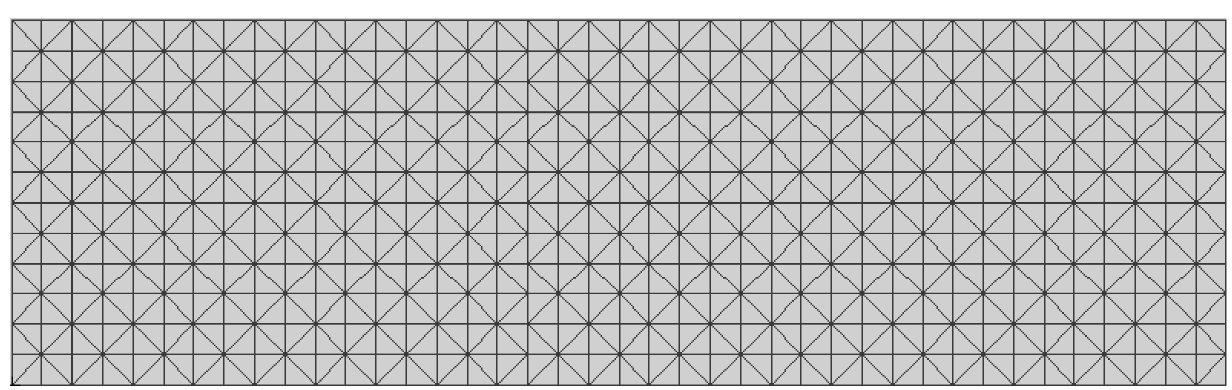

Cohesive Crack Propagation Reveals Quasi-Singular Velocity Field

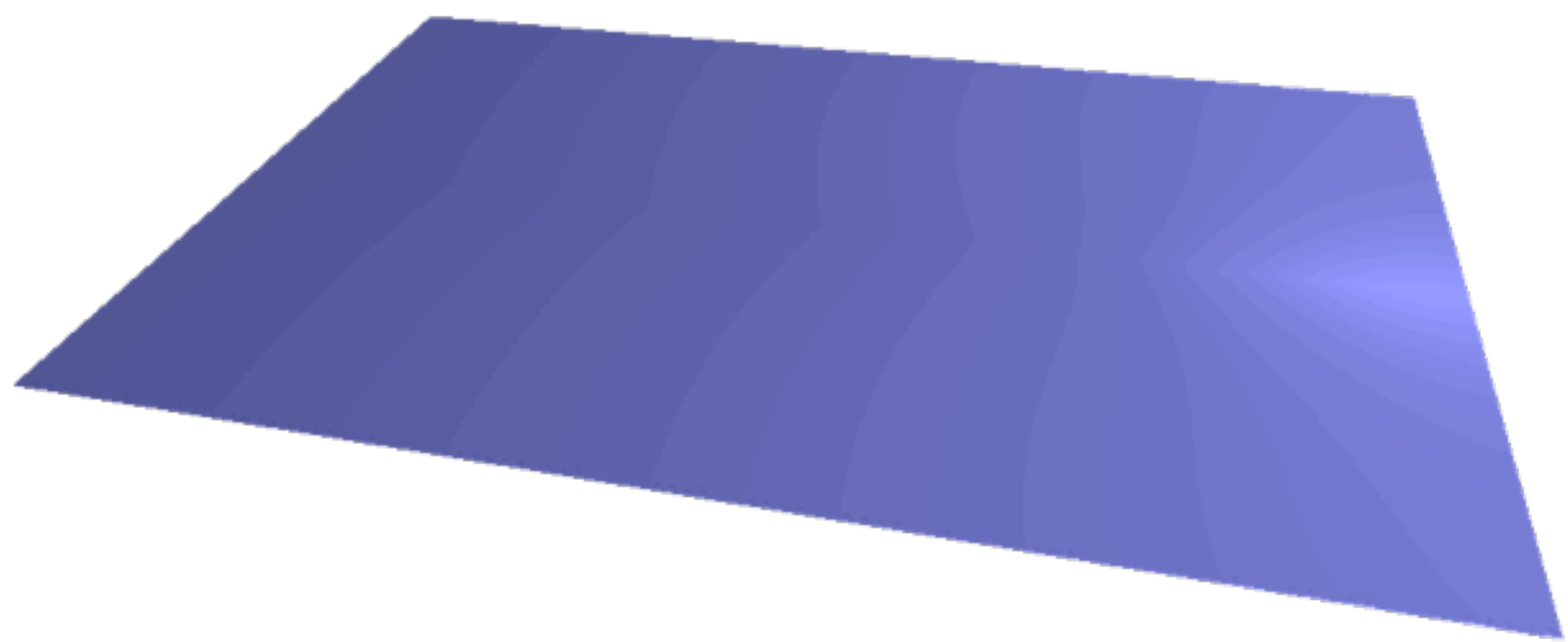

$\sigma_{\mathrm{C}} = 0.1E$

Quasi-singular Material Velocity

Velocity magnitude vs. radial distance from crack tip; t = $4\mu s$

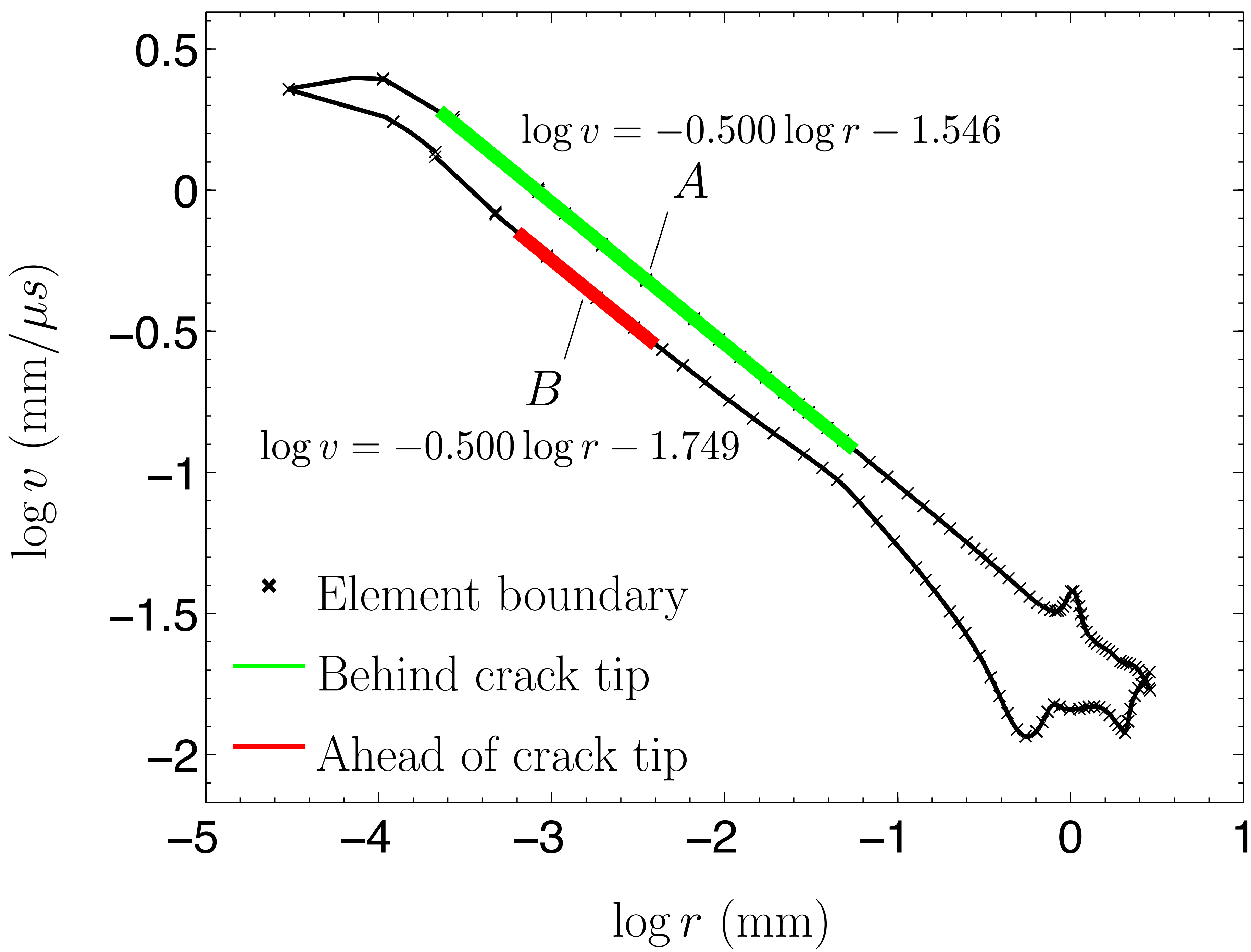

Singular velocity response?

- Verified non-singular core within process zone
- Two length scales (radii): $r_p(t)$ of process zone, and $r_s(t)$ of singular-dominant zone for a sharp crack
- No evidence of singular response when $r_s < r_p$
- Follows singular form where r is in $[r_p, r_s]$ when $r_p << r_s$.

Continuum contact model

Abedi and Haber, "Riemann solutions and spacetime discontinuous Galerkin method for linear elastodynamic contact," CMAME **270** (2014) 150–177.

- Full set of Riemann solutions for frictional contact (separation, contact–stick, <u>contact–slip</u>)
- Isotropic Coulomb friction law
- Eliminates spurious discontinuous response; only separation-to-contact transition requires regularization
- Solutions are free of the usual oscillations
- Characteristic structure is preserved (vs. quasi-static contact conditions)
- Precludes interpenetration without additional constraints
- Models crack closure in SDG fracture models

Square-Plate Impact Example

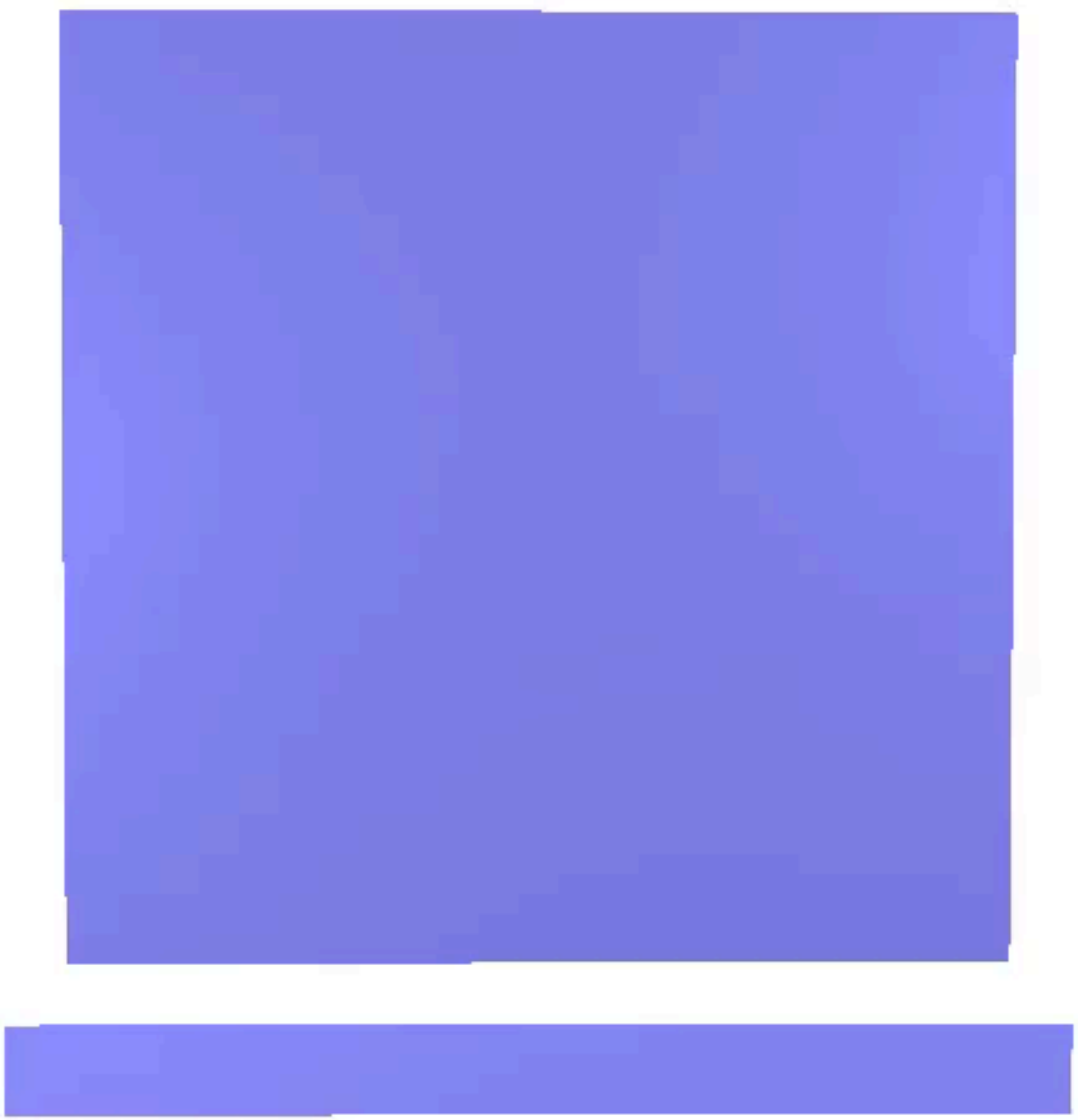

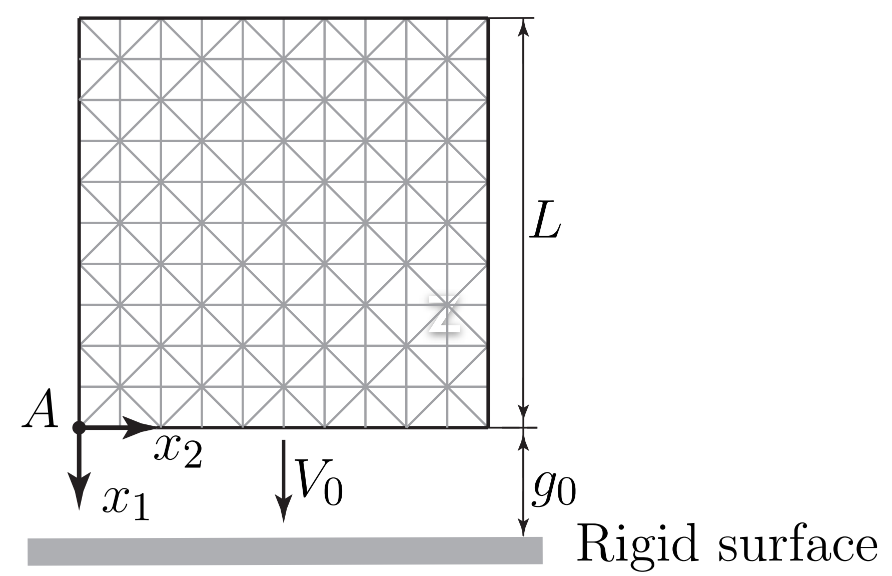

Brake Dynamics Example

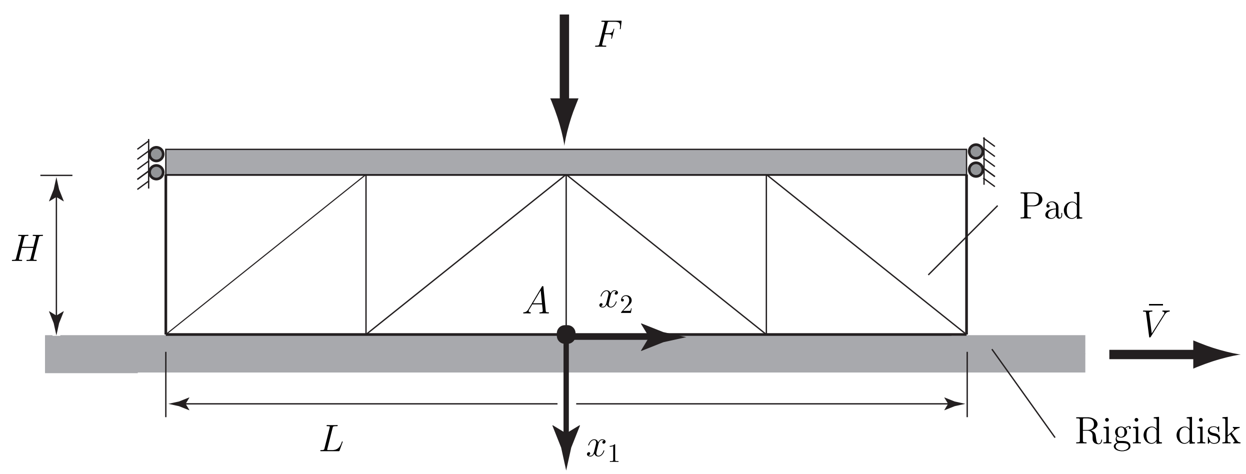

$$E = 10 \text{ GPa}; \nu = 0.3$$

$$\rho = 2000 \text{ kg m}^{-3}$$

$$L \times H = 100 \text{ mm} \times 20 \text{ mm}$$

$$\bar{\sigma}(F) = 1 \text{ MPa}$$

$$\bar{V} = 2 \text{ ms}^{-1}$$

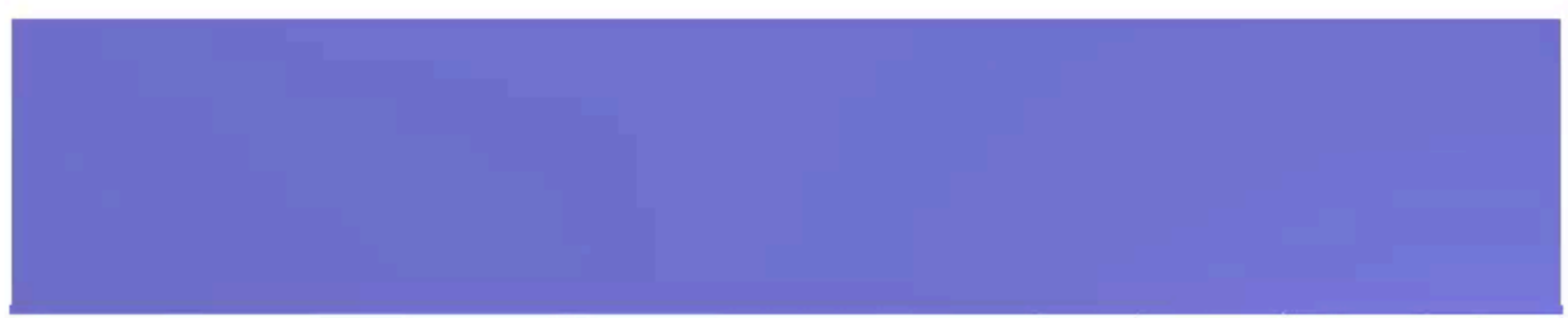

Crack closure: cyclic, mixed-mode, dynamic loading

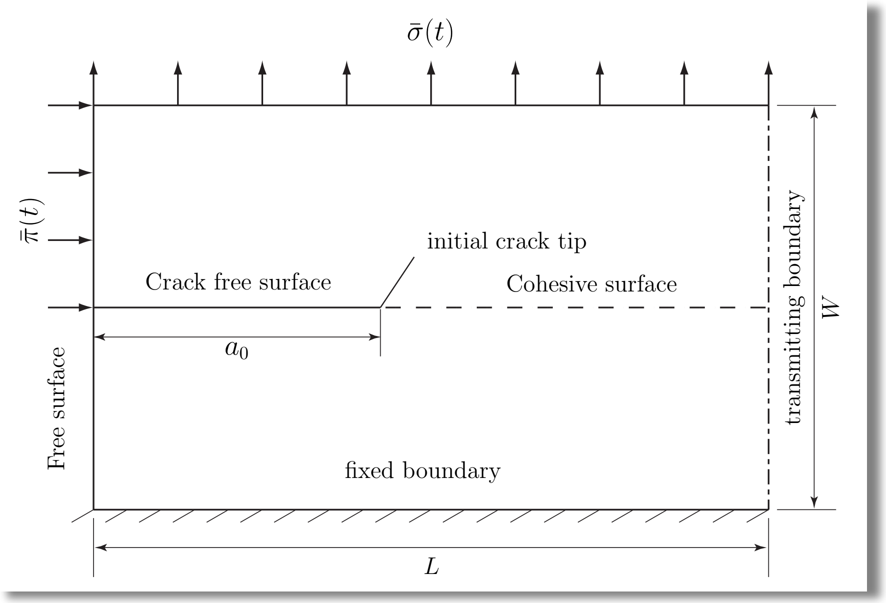

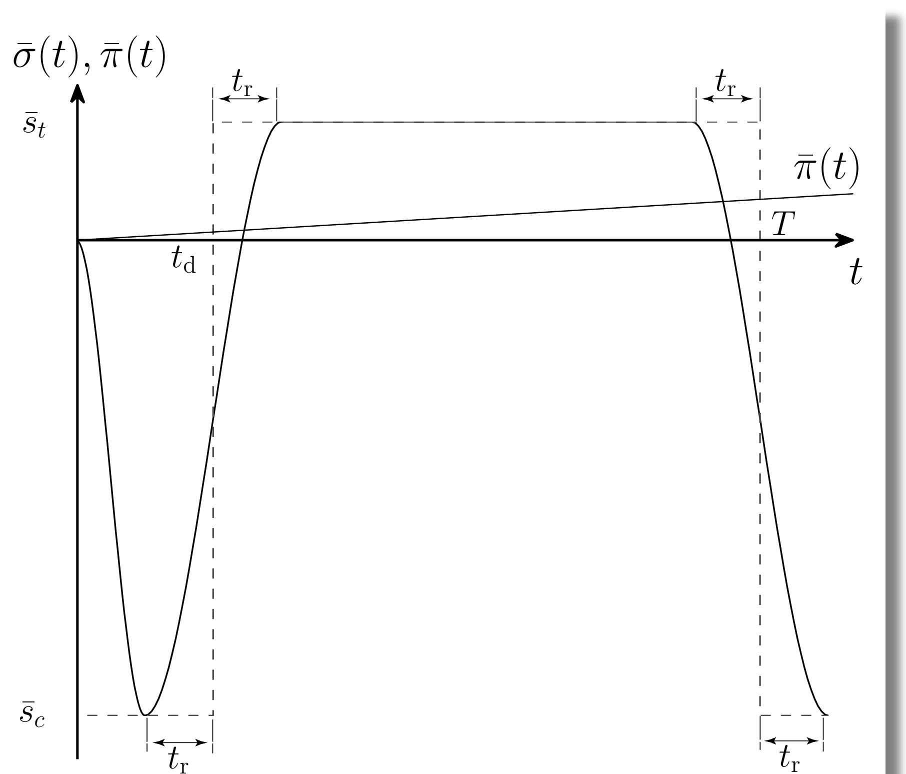

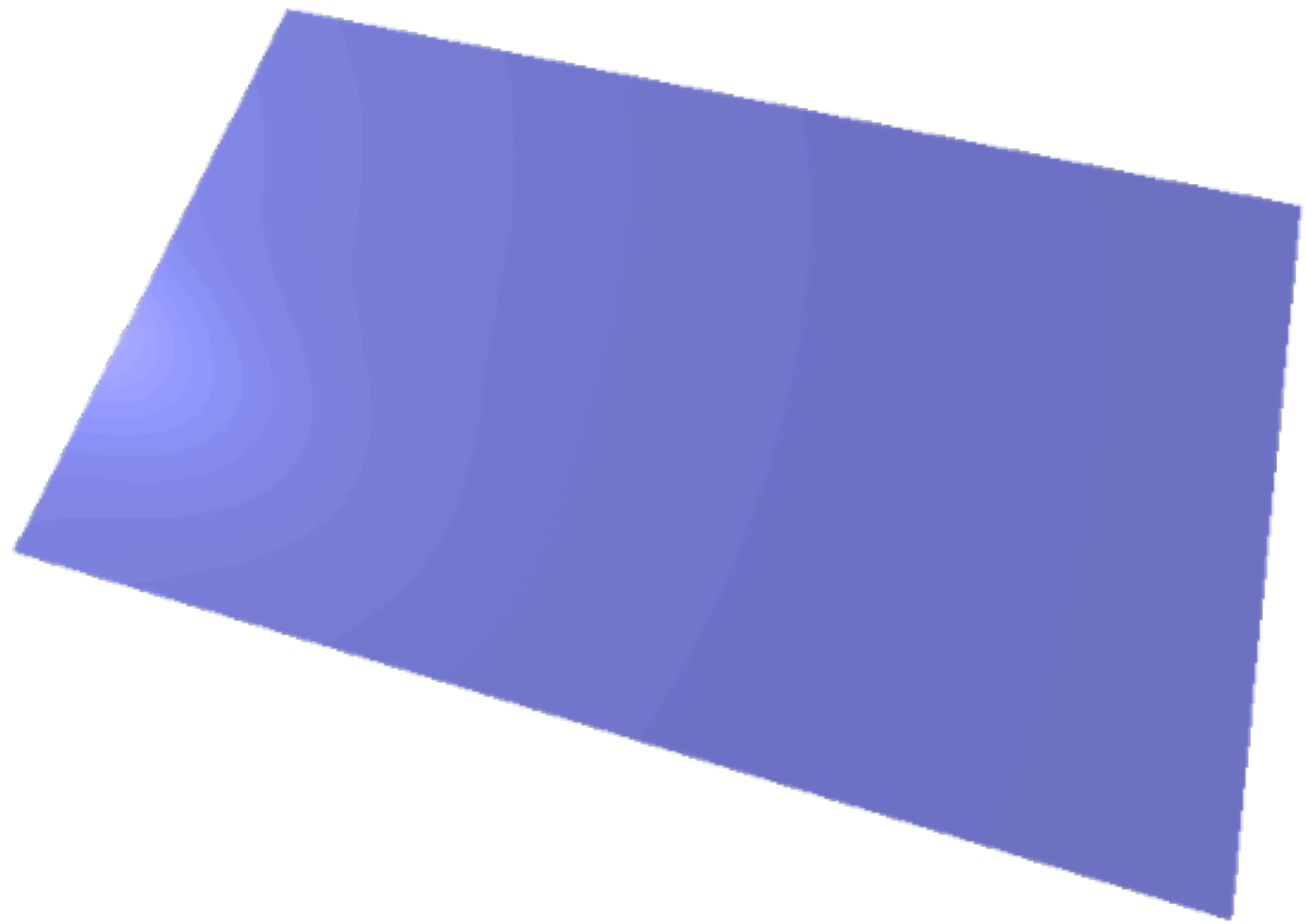

Interfacial damage model for fracture

- Damage parameter φ interpolates between intact (I) and debonded (D) Riemann solutions (debonded case includes separation and all contact modes)

$$\mathbf{s}^* = (1-\varphi)\mathbf{s}_{\mathrm{I}} + \varphi\mathbf{s}_{\mathrm{D}}$$
$$\mathbf{p}^* = (1-\varphi)\mathbf{p}_{\mathrm{I}} + \varphi\mathbf{p}_{\mathrm{D}}$$
$$[\![\mathbf{p}_{\mathrm{I}}]\!] = 0;\ \mathbf{s}_{\mathrm{D}} = 0 \text{ for unloaded, open cracks}$$

- No interfacial stiffness, no traction–separation relation

- Delay damage evolution model with relaxation time τ

$$\dot{\varphi} = \frac{1}{\tau}\min\left(1, \frac{\langle \lambda - \underline{\lambda}\rangle_+}{\bar{\lambda} - \underline{\lambda}}\right)$$

- Probabilistic flaw model nucleates new fracture surfaces

Dynamic fracture with damage-delay *interfacial* failure model

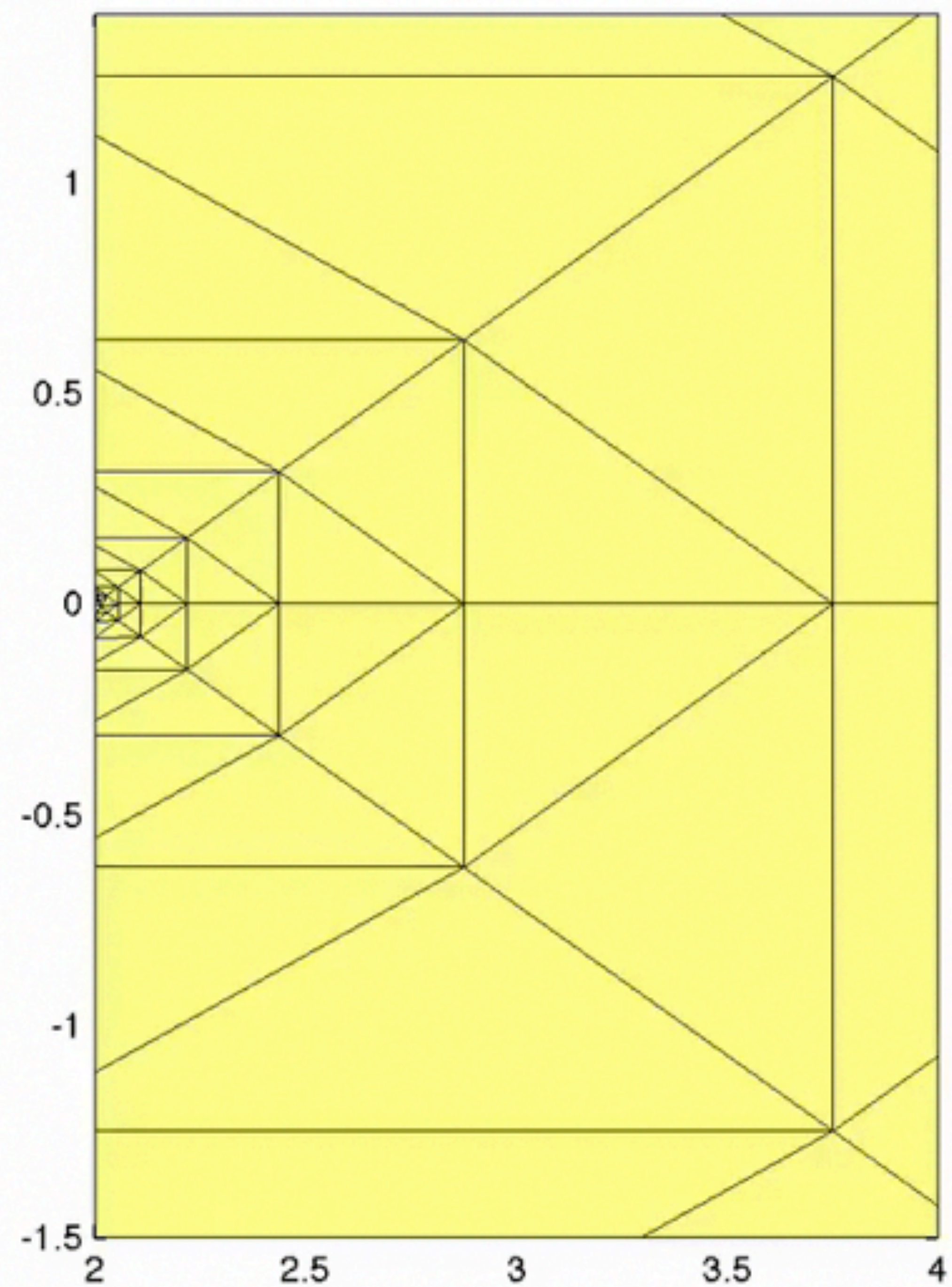

Dynamic fracture with modified damage-delay cohesive model

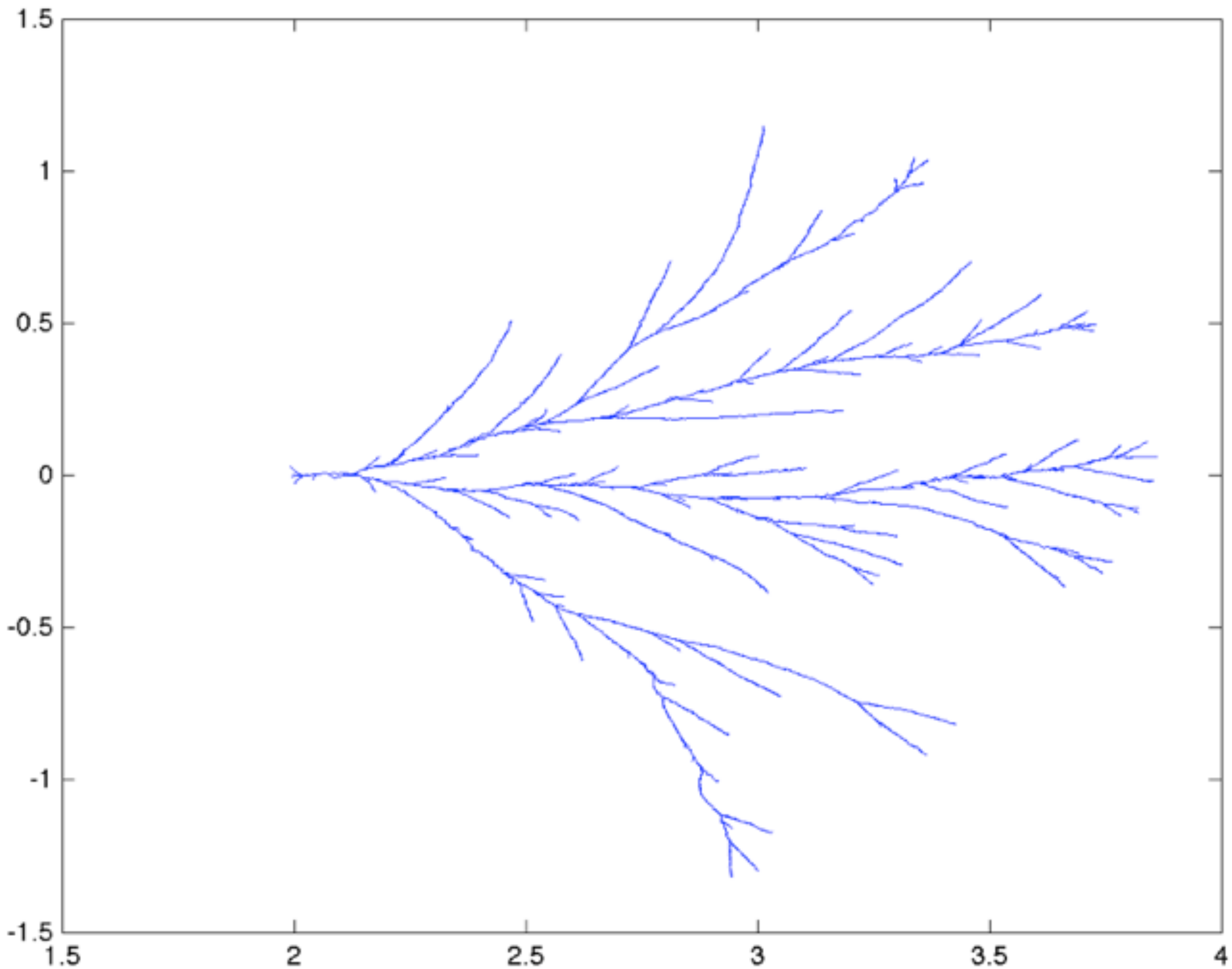

Spall formation under symmetric axial loading

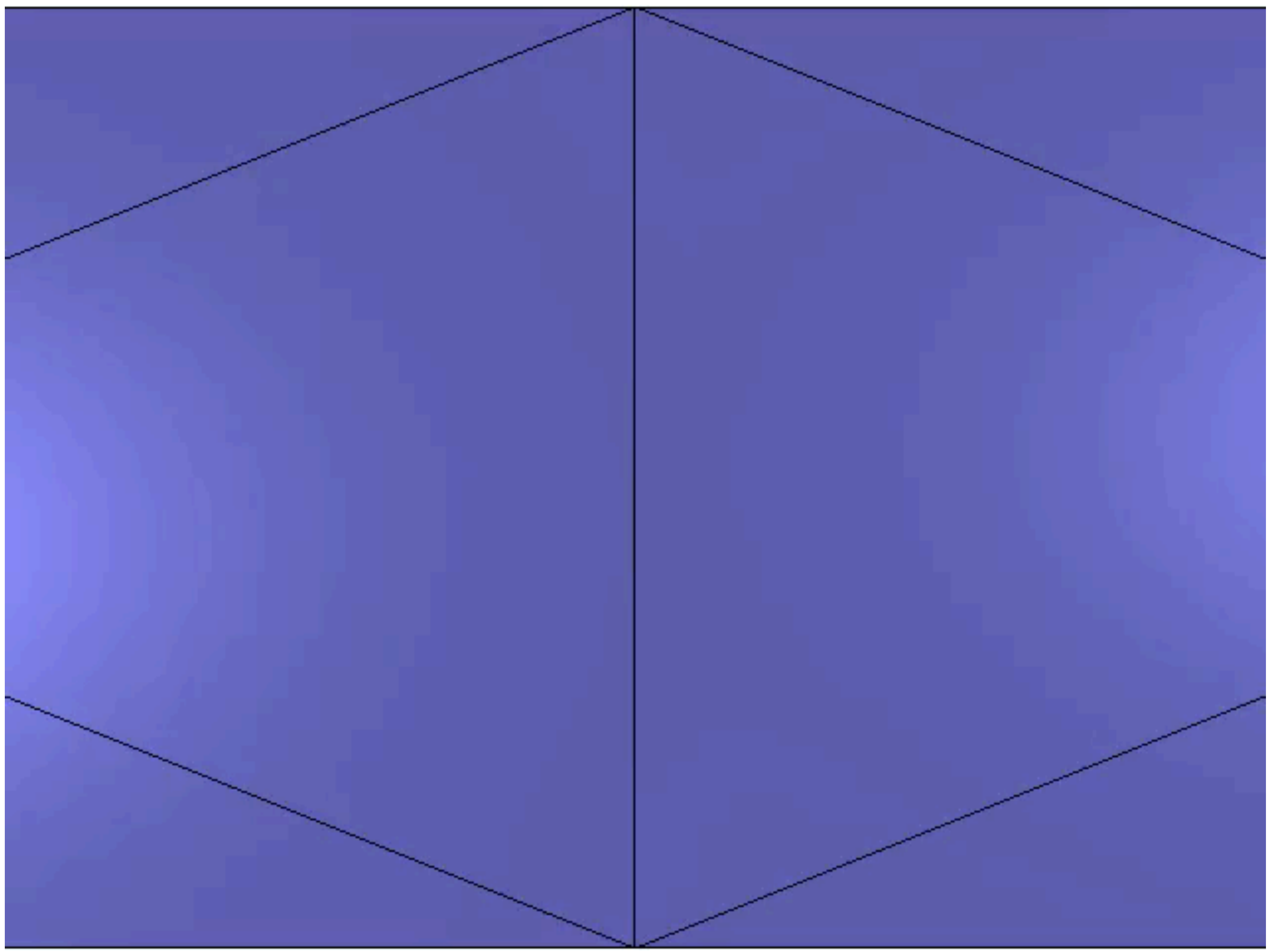

Spall formation under symmetric axial loading

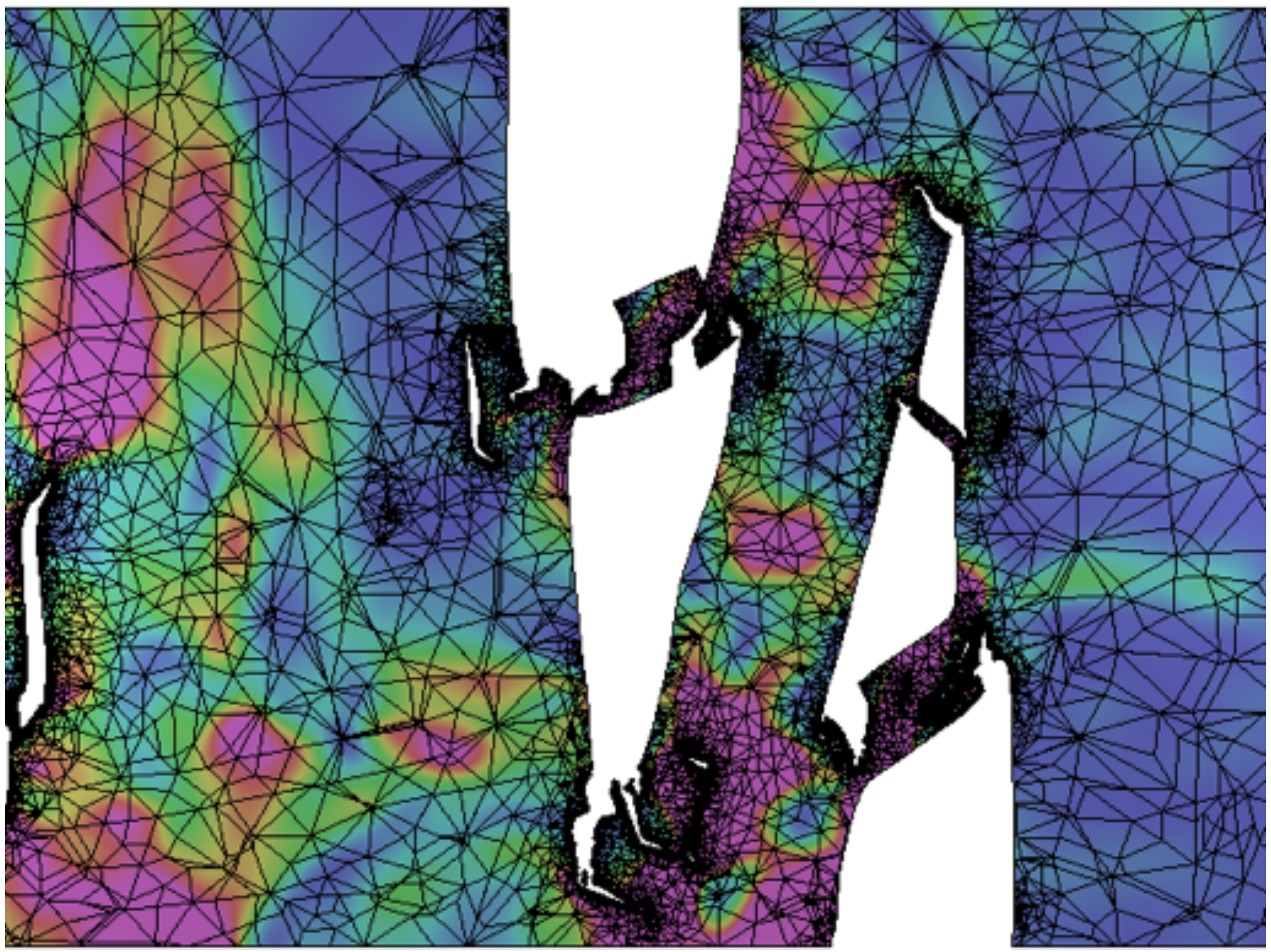

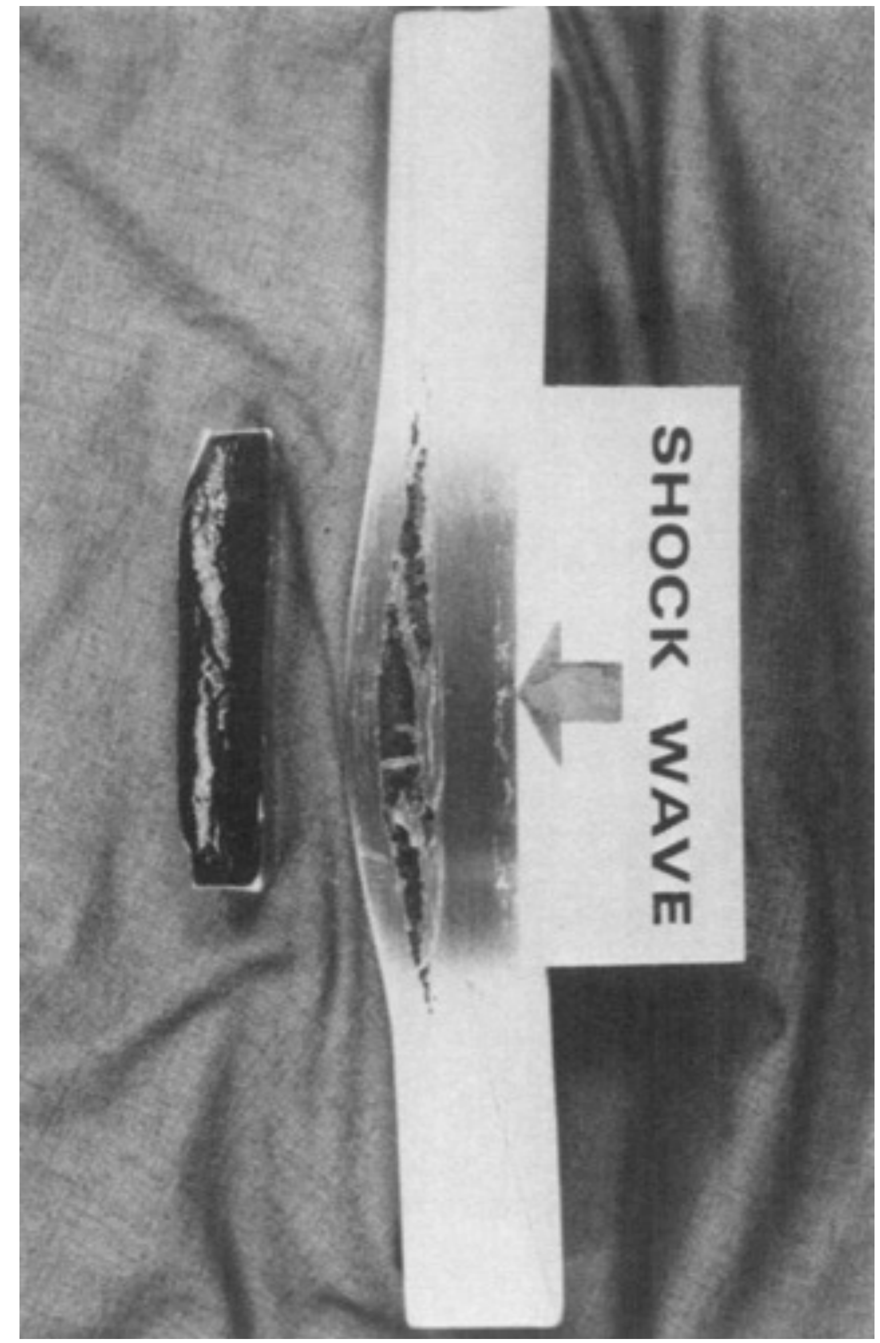

Meyers and Aimone, "Dynamic fracture of (spalling) metals," Prog. Materials Sci. **28**, 1983.

Well bore subjected to ‘explosive’ load

Short-duration, shock-like pulse on bore walls

No initial bore perforations

Well bore subjected to 'explosive' load

Short-duration, shock-like pulse on bore walls

No initial bore perforations

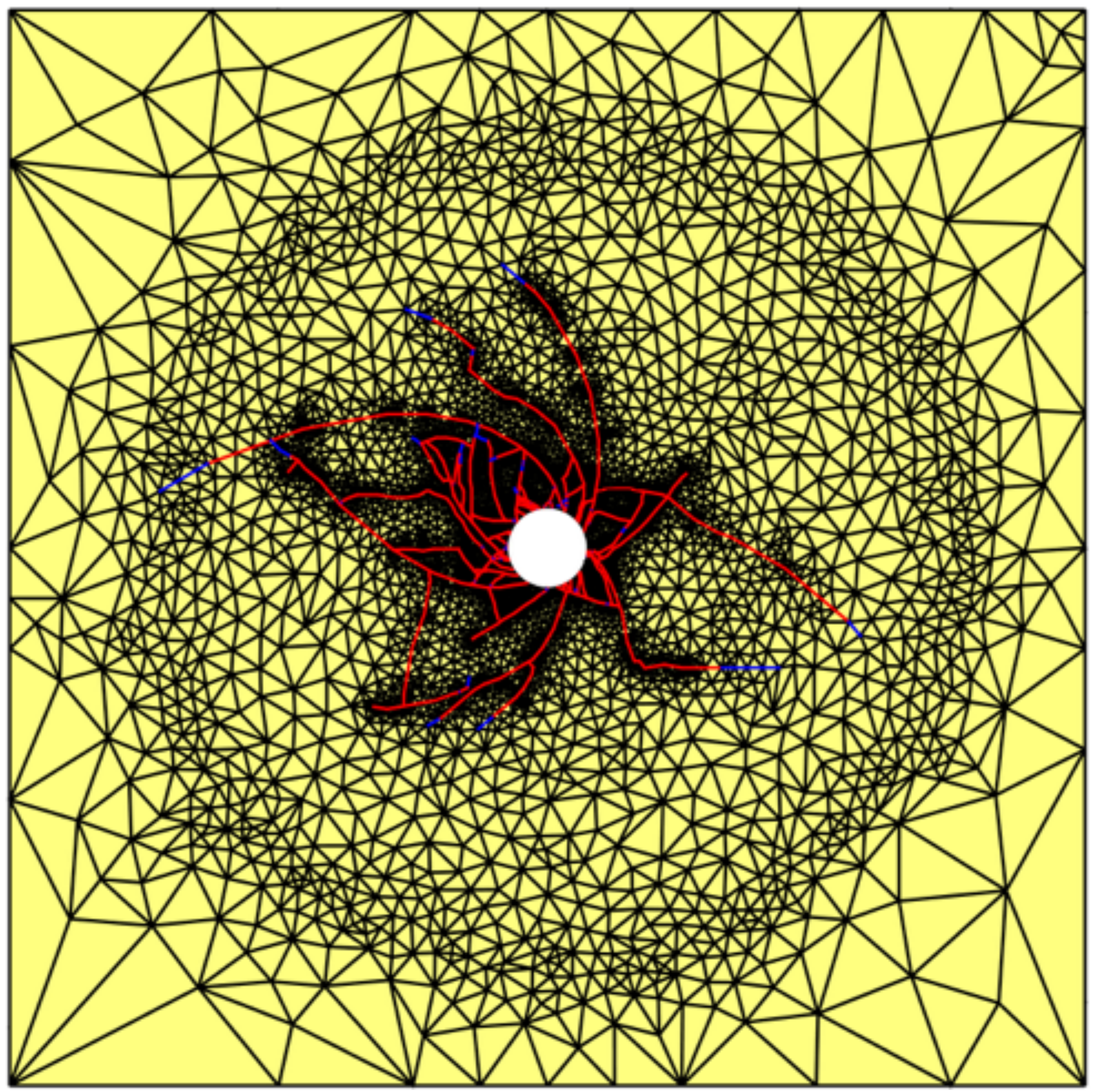

Well bore subjected to fast-ramp load

Bore has four initial perforations

Load ramps to sustained pressure on bore, perforations & cracks

Well bore subjected to fast-ramp load

Bore has four initial perforations

Load ramp to sustained pressure on bore, perforations & cracks

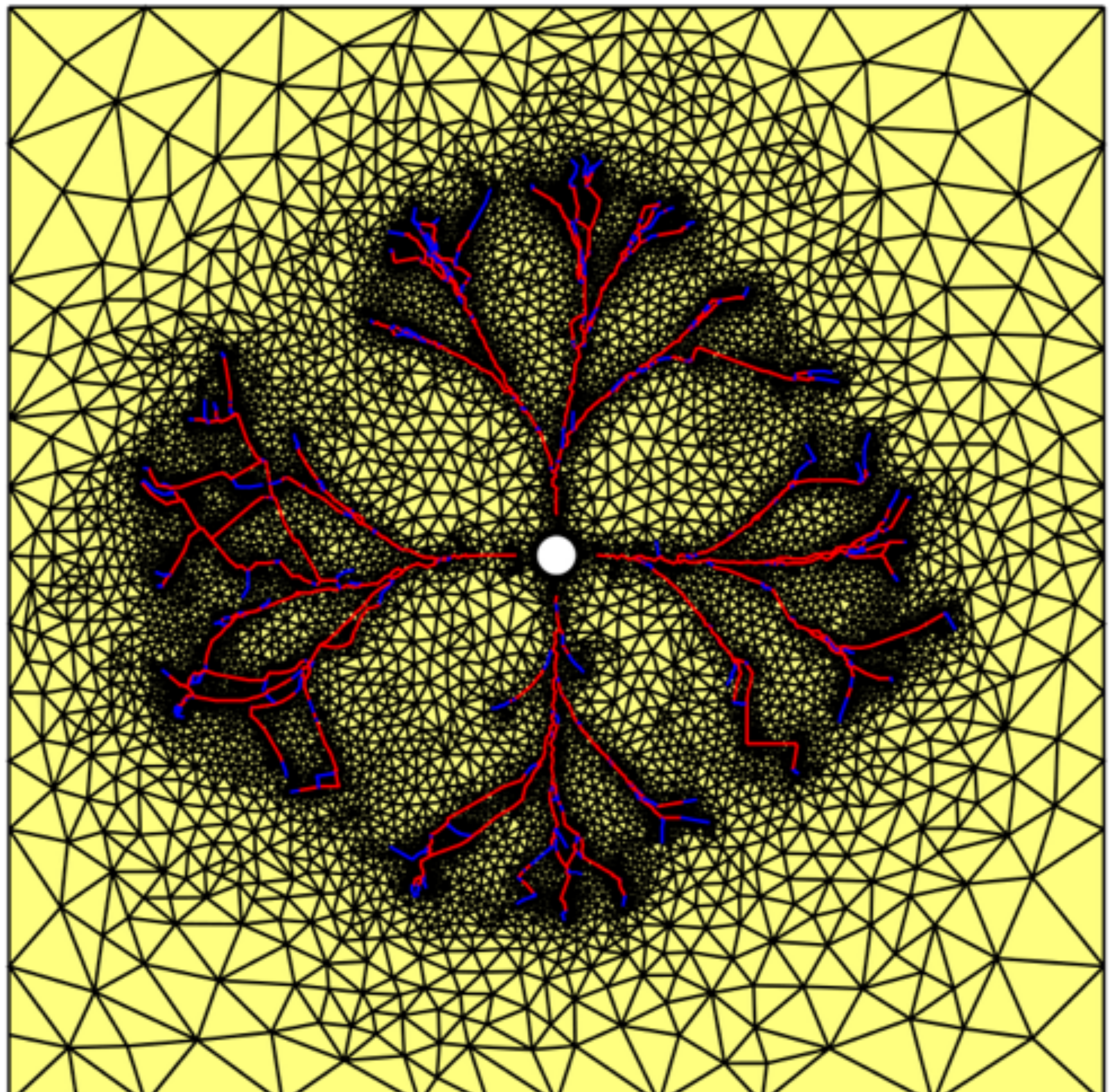

Flaw Orientation Study

Load ramps to sustained pressure on initial horizontal crack

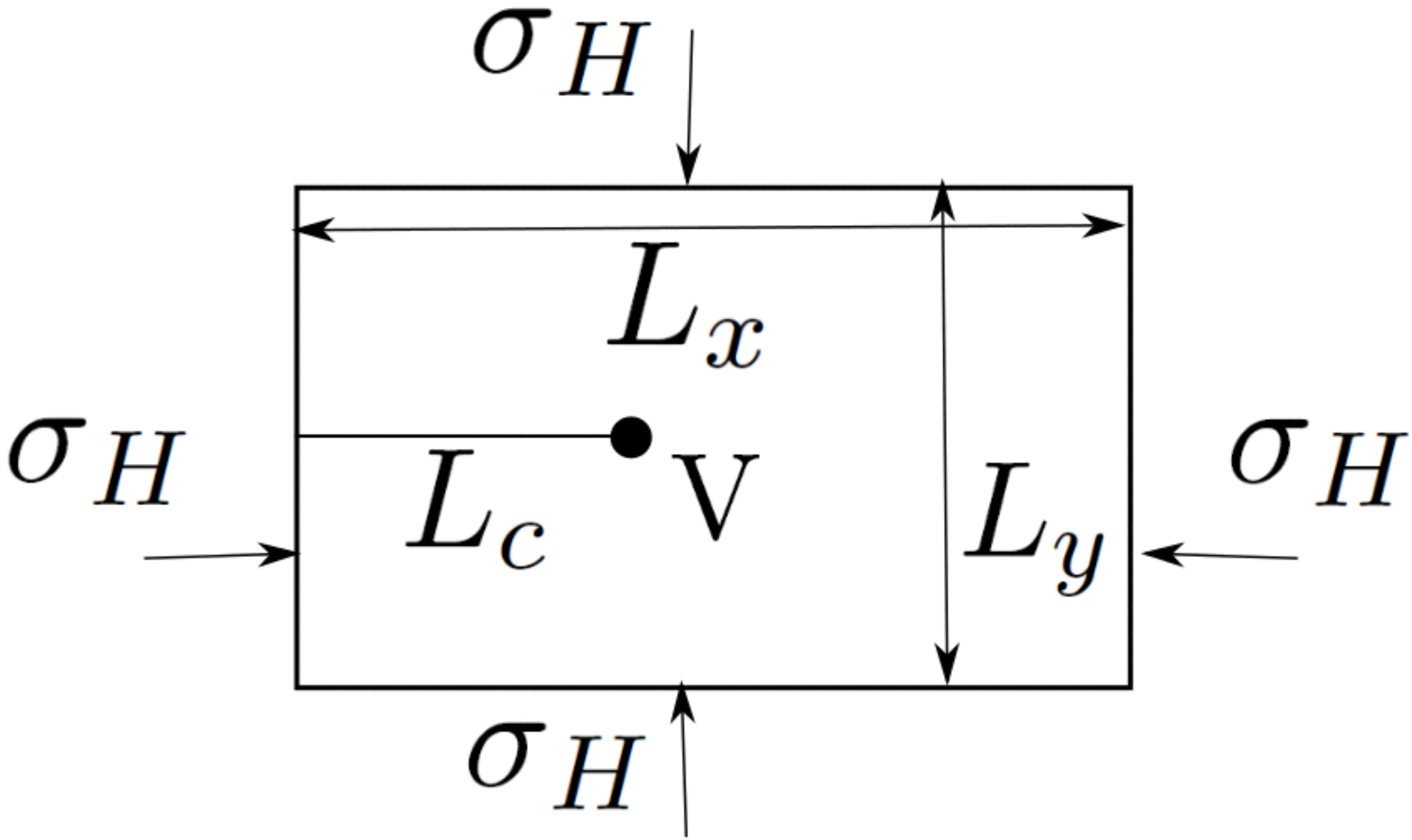

Flaw Orientation Study

Uniform orientation distribution

Load ramps to sustained pressure on initial horizontal crack

Flaw Orientation Study

Probabilistic flaw model biased to 30°

Load ramps to sustained pressure on initial horizontal crack

Conclusions

- Advantages/Disadvantages
  - ★ Excellent performance for strictly hyperbolic problems / can't yet handle systems with elliptic (e.g., quasi-statics) or parabolic equations
  - ★ Rare example where adding dofs (polynomial order, multi-field) in DG improves efficiency.
  - ★ Powerful adaptive meshing capability does not limit order of accuracy
  - ★ Enforcing Riemann solutions improves stability and provides robust mechanism for modeling initial, boundary, contact conditions + fracture
  - ★ Sharp-interface fracture model removes some ambiguities / novel constrained spacetime meshing problem … 3d x time???
  - ★ Asynchronous, embarrassingly parallel structure for HPC
  - ★ Probabilistic nucleation model addresses heterogeneities and offers alternative mechanism for branching

SDG in *3d* x time:
Elastic wave scattering by penny-shaped crack